Tracing the depositional history of Kalimantan diamonds by zircon 2 provenance and diamond morphology studies

by Joko Soesilo

Lithos xxx (2016) xxx–xxx

Contents lists available at ScienceDirect

Lithos

journal homepage: www.elsevier.com/locate/lithos

Tracing the depositional history of Kalimantan diamonds by zircon provenance and diamond morphology studies

Nico Kueter [a,*], Joko Soesilo [b], Yana Fedortchouk [c], Fabrizio Nestola [d], Lorenzo Belluco [d], Juliana Troch [a], Markus Wälle [a], Marcel Guillong [a], Albrecht Von Quadt [a], Thomas Driesner [a]

[a] Institute for Geochemistry and Petrology, ETH Zurich, Clausiusstrasse 25, 8092, Zurich, Switzerland
[b] Faculty of Mineral Technology, State University UPN Veteran Yogyakarta, 52283 Yogyakarta, Indonesia
[c] Department of Earth Sciences, Dalhousie University, 1459 Oxford Street, Halifax, NS, B3H 4R2, Canada
[d] Dipartimento di Geoscienze, Università degli Studi di Padova, Via Giovanni Gradenigo 6, 35131 Padova, Italy

ARTICLE INFO

Article history:
Received 10 November 2015
Accepted 5 May 2016
Available online xxxx

Keywords:
Kalimantan alluvial diamonds
Meratus
Diamond morphology
Diamond radiation coloring
Zircon provenance
Indonesia

ABSTRACT

Diamonds in alluvial deposits in Southeast Asia are not accompanied by indicator minerals suggesting primary kimberlite or lamproite sources. The Meratus Mountains in Southeast Borneo (Province Kalimantan Selatan, Indonesia) provide the largest known deposit of these so-called "headless" diamond deposits. Proposals for the origin of Kalimantan diamonds include the adjacent Meratus ophiolite complex, ultra-high pressure (UHP) metamorphic terranes, obducted subcontinental lithospheric mantle and undiscovered kimberlite-type sources. Here we report results from detailed sediment provenance analysis of diamond-bearing Quaternary river channel material and from representative outcrops of the oldest known formations within the Alino Group, including the diamond-bearing Campanian–Maastrichtian Manunggul Formation. Optical examination of surfaces of diamonds collected from artisanal miners in the Meratus area (247 stones) and in West Borneo (Sanggau Area, Province Kalimantan Barat; 85 stones) points toward a classical kimberlite-type source for the majority of these diamonds. Some of the diamonds host mineral inclusions suitable for deep single-crystal X-ray diffraction investigation. We determined the depth of formation of two olivines, one coesite and one peridotitic garnet inclusion. Pressure of formation estimates for the peridotitic garnet at independently derived temperatures of 930–1250 °C are between 4.8 and 6.0 GPa.

Sediment provenance analysis includes petrography coupled to analyses of detrital garnet and glaucophane. The compositions of these key minerals do not indicate a kimberlite-derived material. By analyzing almost 1400 zircons for trace element concentrations with laser ablation ICP-MS (LA-ICP-MS) we tested the minerals potential as an alternative kimberlite indicator. The screening ultimately resulted in a small subset of ten zircons with a kimberlitic affinity. Subsequent U–Pb dating resulting in Cretaceous ages plus a detailed chemical reflection make a kimberlitic origin unfavorable with respect to the regional geological history. Rather, trace elemental analyses (U, Th and Eu) suggest an eclogitic source for these zircons.

The age distribution of detrital zircons allows in general a better understanding of collisional events that formed the Meratus orogen and identifies various North Australian Orogens as potential Pre-Mesozoic sediment sources. Our data support a model whereby the majority of Kalimantan diamonds were emplaced within the North Australian Craton by volcanic processes. Partly re-deposited into paleo-collectors or residing in their primary host, these diamond-deposits spread passively throughout Southeast Asia by terrane migration during the Gondwana breakup. Terrane amalgamation events largely metamorphosed these diamond-bearing lithologies while destroying indicative mineral content. Orogenic uplift finally liberated their diamond-content into new, autochthonous placer deposits.

1. Introduction

1.1. General introduction

Four alluvial diamond occurrences are known in Indonesian Borneo (Kalimantan): the Sanggau Area in West Kalimantan, diamond deposits in Central and East Kalimantan, and the Meratus area in Southeast

* Corresponding author.
E-mail address: nico.kueter@erdw.ethz.ch (N. Kueter).

http://dx.doi.org/10.1016/j.lithos.2016.05.003
0024-4937/© 2016 Published by Elsevier B.V.

Kalimantan (Fig. 1). Similar to other Southeast Asian diamond occurrences in Phuket (Thailand), Momeik and Theindaw (Myanmar; Griffin et al., 2001; Win et al., 2001), the alluvials containing diamonds from Kalimantan have no associated kimberlite/diamond indicator minerals and their primary source is unknown (Spencer et al., 1988). The setting of the Southeast Asian diamonds within young orogenic belts, interspersed with many suture zones containing (ultra-) high-pressure low-temperature (HP-HT) complexes and ophiolites led to speculations about unconventional (non-kimberlitic) sources for these "anomalous" diamond deposits, especially regarding the largest diamond deposits located in Southeast Kalimantan.

The so-called "headless" alluvial diamonds in comparable geological environments are reported in several young orogenic belts in eastern Australia (Davies et al., 2002), the western USA and Canada (Canil et al., 2005; Casselman and Harris, 2002; Hausel, 2007; Kopf et al., 1990) and the Ural Mountains in Russia (Laiginhas et al., 2009). Their origin is proposed to be linked to (1) subduction of ophiolites into the diamond stability field, (2) exhumed ultrahigh-pressure rocks, or (3) to ancient kimberlite or lamproite sources in which a long alluvial history destroyed all common indicator minerals.

The Southeast Kalimantan diamond occurrences are closely associated with the Meratus Mountains, a northeast–southwest trending collision orogen with prominent ophiolitic units formed in Cretaceous times. Recently, diamonds from chromite pods are increasingly recognized in ophiolites worldwide, reviving the discussion of their significance for the Southeast Asian alluvial diamonds (Nixon and Bergman, 1987; Yang et al., 2014). Similarly, diamonds from the ultra-high pressure metamorphic complexes indicate deep subduction of continental crust, a process that is also considered to have taken place in the late Mesozoic during amalgamation of Central Indonesian continental core (Parkinson et al., 1998). Barron et al. (2008) and Barron et al. (2011) recognized similarities in the Raman-response of the Kalimantan diamonds to subduction-related Copeton–Bingara alluvial diamonds. Graphite pseudomorphs after octahedral diamond were described from peridotites from Beni-Bousera (Morocco; Pearson et al. (1989)) and Ronda (Spain; Davies et al. (1993)). These localities are the classical example of exhumed deep subcontinental lithospheric mantle (SCLM) and Pearson et al. (1989) proposed a similar source for the anomalous diamond deposits in Kalimantan. Based on the trace element data on ultramafic rocks collected in the Meratus area, Monnier et al. (1999) infer that SCLM is present in the region. Smith et al. (2009) determined a suite of mineral inclusions within the Kalimantan diamonds that were typical of a deep peridotitic lithospheric mantle origin with minor eclogite. The plate tectonic reconstructions of Southeast Asia interpreted the presence of diamonds as an indirect evidence for North Australian lithospheric fragments that were dispersed during the Gondwana breakup (e.g. Metcalfe, 1988) and form the continental core of Southeast Asia (Metcalfe, 2011). Taylor et al. (1990) emphasized a Northwest Australian Cratonic origin for the Kalimantan diamonds. These diamonds could have been emplaced either by tectonic emplacement via ophiolite and SCLM obduction during a collisional event, or via post- or syn-orogenic diamond-lifting alkaline magmatic rocks (Bergman et al., 1988; Taylor et al., 1990). Despite an increasing amount of background information, the source rock as well as the timing and geographic location of the emplacement of the Kalimantan diamonds remain unknown.

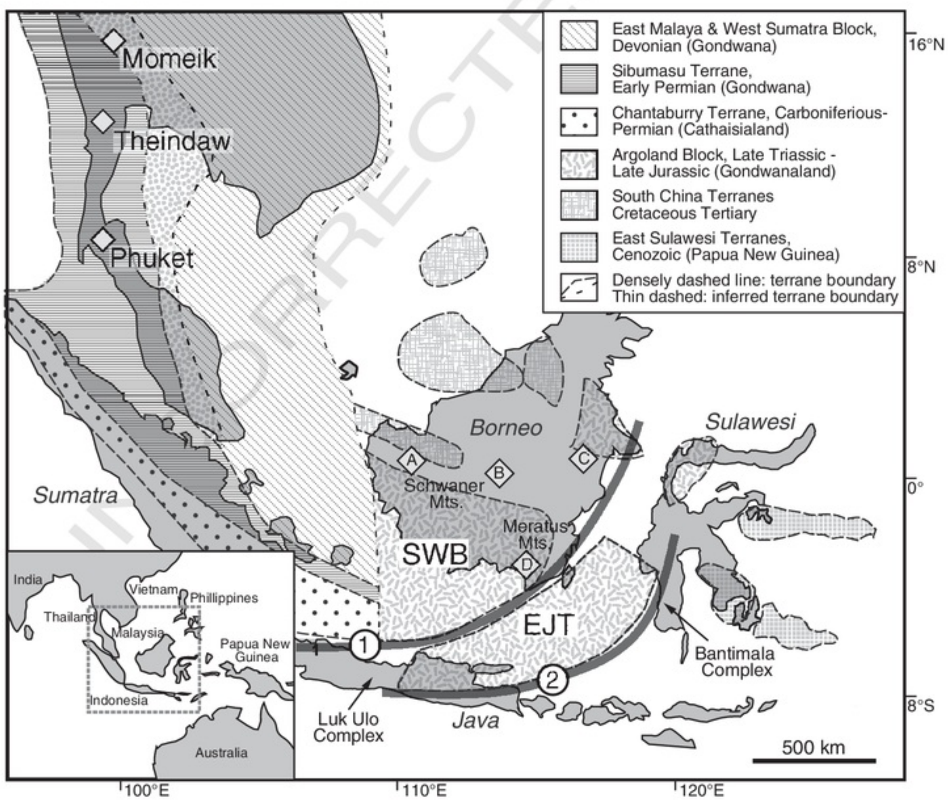

Fig. 1. SE-Asia Geotectonic framework of Southeast Asia modified after Metcalfe (2011). Today's landmasses marked in gray. SWB = Southwest Borneo Terrane, EJT = East-Java West-Sulawesi Terrane, also known as Paternoster Block. The latter two belong to the Argoland Block. Diamond symbols: Alluvial diamond occurrences. A = Sanggau, West Kalimantan, B = Central Kalimantan, C = Kutai Basin, East Kalimantan, D = Cempaka and Meratus Area, Southeast Kalimantan. Bold black lines are inferred paleo-subduction zones. 1 = Karimunjawa trench (active in the Triassic to Jurassic prior collision of EJT terrane with SWB), 2 = Bantimala trench (activation in the Cretaceous after collision of EJT with SWB).

Please cite this article as: Kueter, N., et al., Tracing the depositional history of Kalimantan diamonds by zircon provenance and diamond morphology studies, Lithos (2016), http://dx.doi.org/10.1016/j.lithos.2016.05.003

In this paper, we use the aspects of sediment provenance analysis, an optical study of 332 diamonds and a mineral inclusion study of four diamonds from West and Southeast Kalimantan to (1) elucidate the emplacement and transportation history of Kalimantan diamonds and (2) improve the understanding of the processes that ultimately led to the Meratus orogeny in the Mesozoic era. We focus on diamond-bearing Quaternary and Cretaceous sediments and use the U–Pb dating of detrital zircons combined with trace element screening to identify crystals with mantle affinities, in order to test these as an alternative kimberlite indicator. Combined, zircon-age fingerprints and the observed lack of kimberlite/diamond indicator minerals and results from optical diamond examination are used to derive a source and depositional model for Southeast Kalimantan diamonds.

1.2. Diamond mining

Diamonds in Indonesia mainly occur in alluvial deposits in Kalimantan (Indonesian part of Borneo) where they are found together with gold and platinum in recent or Quaternary river sediments. The center of diamond mining is the Cempaka district, located 50 km east of the province capital Banjarmasin in Kalimantan Selatan (Southeast Borneo). Here, small-scale mining is active today and a professionally operated exploitation of Pleistocene paleo-river alluvium was conducted until 2009 by the company *PT-Galuh Cempaka*. Smaller diamond occurrences are known from the Sanggau area in West Kalimantan (Kalimantan Selatan) and Central and East Kalimantan (Smith et al., 2009). The publications of Koolhoven (1935), van Bemmelen (1949) and Spencer et al. (1988) provide excellent information and details on the mining and exploration history of Kalimantan diamonds.

1.3. Geological overview

The continental core of Central Indonesia (Java, Kalimantan and West Sulawesi) consists of a continental fragment (Argoland, Metcalfe, 2011) that was separated from the northwestern Australian margin in the Early Mesozoic (Fig. 1). It is comprised of at least four smaller parts: Semitau-Terrane, Southwest-Borneo-Terrane (SWB), East-Java-Terrane (EJT, also known as Paternoster-block in other publications), and West-Sulawesi-Terrane (Hall and Sevastjanova, 2012; Metcalfe, 2011). Subsequent terrane-amalgamation against a growing Southeast Asian Peninsula (Sundaland) was accompanied by the closure of an old subduction zone, the activation of a new subduction zone associated with episodes of calc-alkaline magmatism, and the emplacement of ophiolites. The East-Java-terrane is framed by two tectonic sutures with associated ophiolites and high-pressure low-temperature (HP–LT) metamorphic terranes containing blueschists and eclogites. A Jurassic accretionary complex extends from the Java Sea towards the Meratus Mountains and bends northwards to the Mangkalihat peninsula of Kalimantan Timur, forming the suture between the Southwest-Borneo-Terrane and the East-Java-Terrane (Karimunjawa trench; Fig. 1). A second Cretaceous accretionary complex is represented by UHP-mélanges and ophiolites in Karangsambung (Central Java), Bantimala and Barru (Southeast Sulawesi) and Latimojong and Pompangeo (Central Sulawesi) and forms the suture between the East-Java-Terrane and the West-Sulawesi-Block (Bantimala trench; Fig. 1) (Baese, 2013; Parkinson et al., 1998; Soesilo, 2012, 2015).

The southern Meratus can be subdivided into five major units (Fig. 2) as follows: (1) the metamorphic basement, (2) an ophiolite complex, (3) crosscutting calc-alkaline magmatic bodies, (4) Late Cretaceous sediments covering the basement, and (5) unconformably overlying Cenozoic sediments (Sikumbang, 1986; Sikumbang and Heryanto, 1994). Toward the east the metamorphic basement changes from greenschist-facies metamorphic grades into granulite-facies rocks (peak conditions 12 kbar and 900 °C, Soesilo, 2012), with metamorphic ages ranging from the Lower Jurassic to the Lower Cretaceous (Parkinson et al., 1998; Soesilo, 2012). The prominent Meratus ophiolite (2) comprises the large eastern Manjam Range and the smaller western Bobaris Range. The ultramafics are mostly heavily tectonized and serpentinized, especially along the Bobaris Range, but some localities provide fresh peridotites. The Manjam Range hosts (leuco-) gabbroic bodies, some of which are believed to be associated with the peridotites (Sikumbang, 1986). Mafic ophiolite constituents in both ranges appear mostly non-metamorphosed or of greenschist-facies grade. The ophiolite-formation episode including obduction was constrained between the Permo-Triassic to Early Cretaceous, based on radiolaria geochronology, radiogenic ages obtained from ophiolite-hosted platinum-group minerals and low-grade metamorphic mica schist intercalating the ophiolite (Coggon et al., 2011; Parkinson et al., 1998; Wakita et al., 1998). Calc-alkaline intrusions (3) cutting ophiolites and metamorphic basement have co-genetic volcanic products forming the massive volcaniclastic deposits of the Pitanak Group (4) (Sikumbang, 1986; Sikumbang and Heryanto, 1994; Yuwono et al., 1988). The oldest autochthonous sedimentary strata (4), the Aptian to Early-Cenomanian Batununggal limestones, diminish with the onset of Meratus rise in the Cenomanian. Batununggal limestones occur in only few localities but olistoliths and carbonate-debris are frequently found in the younger sediments. Clastic sediments of the Alino Group and volcaniclastic sediments of the Pitanak Group become the predominant sedimentary facies. Coal-rich Eocene flysch-type sediments (5) unconformably cover the Mesozoic basement (Witts et al., 2012).

1.4. Upper Cretaceous stratigraphy and diamond occurrences

Upper Cretaceous ages of all formations of the Mesozoic autochthonous sediments are mainly based on the (micro-)fossil record including palynology, mollusk and micro-fauna (Hashimoto and Koike, 1973; Sikumbang, 1986). Over the past decades, a number of workers profoundly revised the order of the sedimentary units resulting in confusing terminology and age constraints. Fig. 2. provides a simplified stratigraphic column based on the work of Sikumbang (1986) and the newest geological map (Banjarmasin Quadrangle 1712, Sikumbang and Heryanto, 1994).

The oldest known sediments, fossil-rich limestones of the Batununggal Formation, represent shelf to near-shore sediments. The Eastern Manjam ophiolite is predominantly covered by flysch-type sediments of the Cenomanian to Maastrichtian Pudak/Pitap Formation (two names existent). Carbonate and ophiolite olistoliths of up to 2 km size and chaotic sequences of sedimentary mélanges might record times of high seismic activity (Festa et al., 2010; Sikumbang, 1986). Early diamond explorers noted the lack of diamond in the rivers draining the eastern Manjam ophiolite and the overlying Pudak/Pitap sediments (Koolhoven, 1935).

The claystones and clay sandstones of the Paniungang Formation occur along the river Sungai Paniungang in the central Meratus and at the Southeast flank of the southern Meratus. As a minimum age for these sediments, Sikumbang and Heryanto (1994) constrain a Cenomanian age and infer a low energy depositional environment (e.g. shelf). Early explorers drew no links between the local diamond occurrences and the Paniungang Formation (Koolhoven, 1935; van Bemmelen, 1949). However, villagers from a small settlement (Sumber Baru) at the river Paniungang report occasional diamond findings in soil and river bedload.

The Keramaian Formation is an Early Campanian turbidite sequence of volcanic sandstones and mudstones that are intercalated by radiolarian cherts. The formation is present along the western margin of the Meratus and is in contact with the Bobaris ophiolite and the calc-alkaline volcanics of the Pitanak Group. No direct association to diamonds is reported.

The alluvial conglomerates and sandstones of the Manunggul Formation represent the most prominent Cretaceous strata and are located in the central to the northern part of southern Meratus. They partly overlie the ophiolites and the metamorphic basement and

Please cite this article as: Kueter, N., et al., Tracing the depositional history of Kalimantan diamonds by zircon provenance and diamond morphology studies, Lithos (2016), http://dx.doi.org/10.1016/j.lithos.2016.05.003

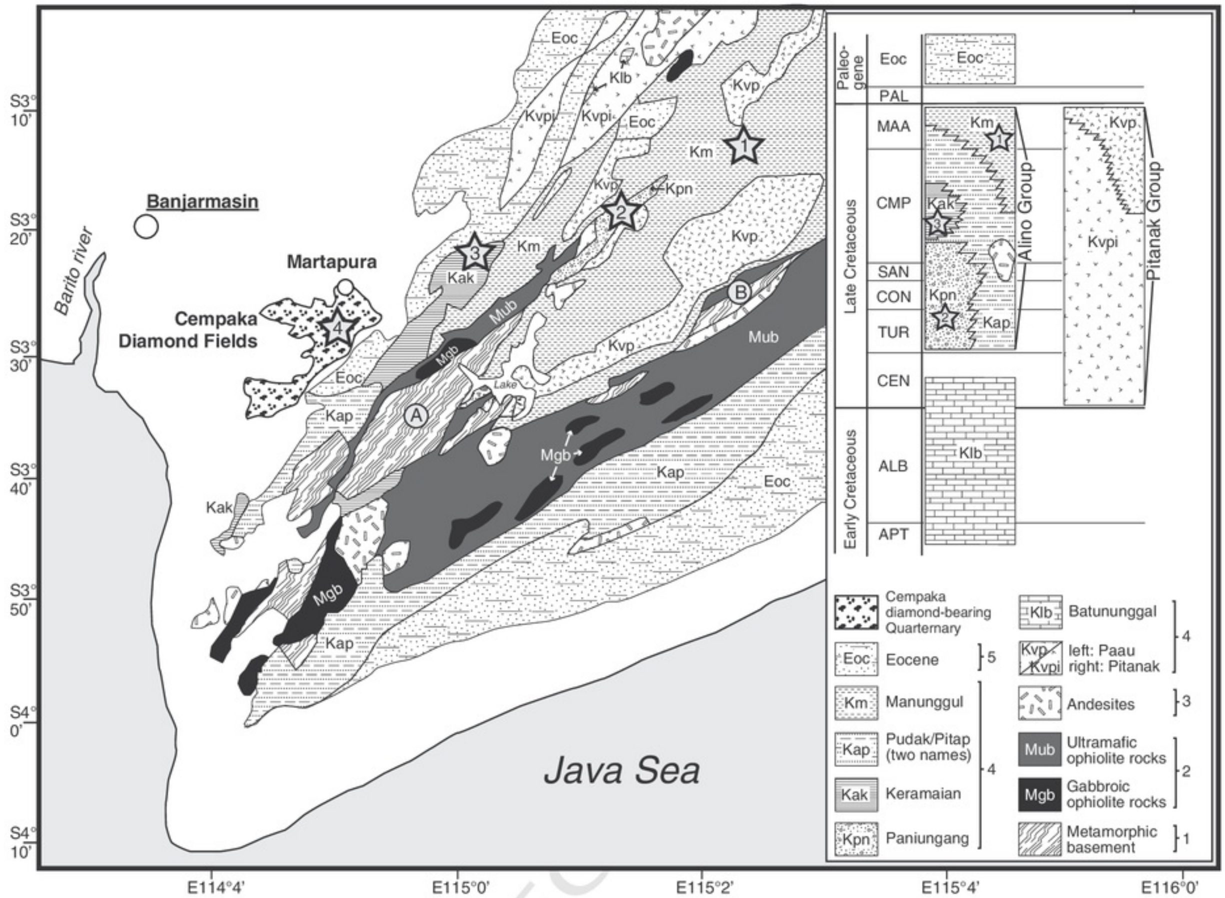

Fig. 2. Meratus Geological map and stratigraphic column of the Cretaceous sediments of the South Meratus after Sikumbang (1986) and Sikumbang and Heryanto (1994). Stars indicate sample localities: 1 = Manunggul formation (sample M3 and IK22-8), 2 = Paniungang formation (IK20-1) and volcaniclastic Paau formation (IK21-1). 3 = Keramaian formation volcaniclastic sandstone (IK9-1), 4 = Keramaian formation turbidite (IK8-1), 5) Cempaka Quatenary paleo-channel heavy mineral concentrate (provided by PT-Galuh Cempaka). The circles: A = locality of Hauran/Aranjo schist (165–190 Ma and 110–119 Ma muscovite K–Ar age ranges, Wakita et al., 1998), B = Central Meratus garnet granulites (135–154 Ma U–Pb SHRIMP-age ranges of zircon, Soesilo, 2012). Numbers 1 to 5 in the key refer to the geological overview in Section 1.3.

contain debris of all aforementioned formations. Sikumbang (1986) suggests a pull-apart basin acting as a collector for debris from the surrounding Meratus Mountains during the Campanian to Maastrichtian. The base of the Manunggul Formation was subdivided by Sikumbang (1986) into the lower polylithic conglomerates of the Pamali Member and the predominantly volcaniclastic conglomerates of the Benuariam Member. The Pamali Member has early been recognized as a secondary (sedimentary) source for the local diamonds and rivers draining the Manunggul Formation were generally reported as diamond-bearing in the literature (Koolhoven, 1935; Krol, 1920; Spencer et al., 1988) and during our field-campaign.

2. Methods and material

2.1. Samples

We bought 332 diamond crystals from artisanal miners from the two most important diamond deposits of Kalimantan: (1) the Cempaka district (Spencer et al., 1988) and rural areas within the Meratus Mountains (situated in the district Kalimantan Selatan, sample suite "KS", $n = 247$) and (2) West Kalimantan (Sanggau area situated in the district Kalimantan Barat, sample suite "KB", $n = 85$). These sample localities correspond to the diamond symbols A and D respectively in Fig. 1. The diamonds were selected randomly without applying any quality criteria to avoid artificial bias and collect representative samples.

Zircon grains were recovered from rock samples of c. 2 kg each. The location of the outcrops chosen according to the literature (Koolhoven, 1935; Krol, 1920; van Bemmelen, 1949) and the Sikumbang and Heryanto (1994) geological map (Banjarmasin Quadrangle 1712) include: sandstone of the Paniungang Formation (IK20-1), sandstones and conglomerates of the Manunggul Formation (samples IK22-8, M3), turbidite siltstone of the Keramaian Formation (IK8-1), and two volcaniclastic sediments sampled from the Keramaian Formation (Alino Group, IK9-1) and the Paau Formation (Pitanak Group, IK21-1). A 5 kg heavy mineral concentrate from exploration drilling into a Pleistocene paleo river channel in the western Meratus lowlands was kindly provided by the alluvial diamond mine PT-Galuh Cempaka. A table with sample localities, brief description and the diamond context can be found in the Electronic Appendix 2.

2.2. Analytical methods

The samples were electro-crushed using a Selfrag, and heavy minerals were separated from the 65–355 μm sand fraction via standard heavy mineral separation procedures (Mange and Maurer, 2012) with bromoform or acetone-diluted methylene iodide (both

Please cite this article as: Kueter, N., et al., Tracing the depositional history of Kalimantan diamonds by zircon provenance and diamond morphology studies, Lithos (2016), http://dx.doi.org/10.1016/j.lithos.2016.05.003

$\rho = 2.8$ g/cm^3). The concentrate was optically screened for kimberlite indicator minerals, all garnets, glaucophane, and zircon. A milligram-sized fraction of the heavy mineral concentrate was magnetically cleaned from ferromagnetic particles and mounted on glass slides with piperine as the optical medium (Martens, 1932) for qualitative microscopic investigations. A fraction of 522 macro-sized zircons (>355 μm) was additionally recovered from the Pleistocene heavy mineral concentrates for a separate screening for kimberlite zircons.

Descriptions of zircon morphology for all dated crystals followed the approach of Witts et al. (2012). Zircons and garnets were separated randomly from the heavy mineral concentrates, mounted and polished. Cathodoluminescence-imaging (CL) of the inherited cores and growth patterns in zircons chosen for dating was done on a FEI Quanta 200 FEG scanning electron microscope at the Scientific Center for Optical and Electron Microscopy (ScopeM) at ETH Zurich.

Trace-element analyses and U–Pb dating on zircon were performed on a Resonetics Resolution S155-LR laser ablation system coupled to an Element XR (Thermo Fisher) ICP MS using spot sizes of 30 μm, a laser pulse rate of 5 Hz and an energy density of 2.5 J/cm^2 at the sample surface. Ablation spots for U–Pb dating were set on outer growth zones in order to obtain the youngest crystallization age. Trace elements were measured directly next to previous ablation craters for dating in the same growth zone. Ablation spots for trace elements on non-dated zircons were set randomly on the polished surface. NIST SRM 612 was used as a primary standard for trace element analysis.

The GJ-1 zircon served as the primary age standard whereas Mud Tank carbonatite and Plešovice granulite zircon (Hanchar and Hoskin, 1998; Sláma et al., 2008) were used as a secondary standard for data quality control. Only concordant ^{206}Pb/^{238}U vs. ^{207}Pb/^{235}U ages with ratios in-between 0.9 and 1.1 were used for provenance interpretation. The zircon ages reported in the following are ^{206}Pb/^{238}U ages with a 2σ uncertainty. Data reduction was done using the software-packages IOLITE (www.iolite-software.com) and SILLS (Guillong et al., 2008).

Major element composition of garnets and amphiboles were analyzed with a JEOL JXA-8200 electron microprobe (EPMA) at ETH Zurich. Detailed information on standards and analytical setup can be found in the electronic supplementary material. Carbon-coated samples were measured with 20 nA electron beam current, 15 kV acceleration voltage and 1 μm spot size. The counting times were 20 s on the peak and 10 s on the background. All chemical analysis and age dates can be found in the Electronic Appendix 1 of this publication.

The optical description of the diamonds was conducted with a reflected light microscope and a stereo microscope with a daylight source. Table 2 in the Electronic Appendix 2 provides the description scheme for the abrasion feature evaluation. Additionally, Electronic Appendix 2 contains a scheme modified from McCallum et al. (1991) for distinguishing between dodecahedral and tetrahexahedral (THH) diamonds as applied in this study.

Four diamonds (CEM 61, CEM 161, CEM 152 and KB 52) showed mineral inclusions suitable for an in-situ single-crystal X-ray diffraction investigation. The measurements were performed at the Department of Geosciences of University of Padova using a recent prototype instrument constituted by a Supernova single-crystal diffractometer equipped with an X-ray micro-source working at 50 kV and 0.8 mA, beam size about 0.11 mm (Rigaku-Oxford Diffraction) and with a zero noise 200 K Pilatus detector (Dectris). The sample-to-detector distance was 68 mm. In detail, we have investigated six inclusions, four olivines, one coesite and one peridotitic garnet. Complete intensity data collections were performed for the four olivines and the garnet in order to determine their chemical compositions (Angel and Nestola, 2015) and apply elastic geobarometry methods (see Nestola (2015) for a review). For coesite this was not necessary due to its pure SiO_2 composition. Because the inclusions are buried inside the diamond, the X-ray diffraction method allowed determination of their chemical composition without needing to destroy the diamond to expose inclusion for electron microprobe analysis. Intensity data were collected up to $2\theta° \approx 65°$ for all inclusions and the crystal structure refinements were based on the electron-in-bond model with scattering curves for ionized atoms in order to obtain accurate compositions (Angel and Nestola, 2015). Final structural data were deposited with the journal as CIF files (see Electronic Appendix 3). For all refinements the agreement factor R_1 was below 0.025 indicating very-high quality data.

3. Results—Sediments

3.1. Petrography and qualitative heavy mineral analysis

Sample IK20-1 from the Paniungang Formation is a badly sorted, grain-supported immature sandstone with mainly angular to sub-angular lithoclasts and minor rounded sedimentary constituents. Lithoclasts are predominantly angular to sub-angular fragments of andesites, elongated fragments of muscovite schist with bands of tectonized quartz, sub-rounded radiolarites sometimes with internal brecciation, and elongated plastically deformed claystone clasts. Monocrystalline fragments consist of angular to subangular hornblende, plagioclase, K-feldspar and rounded quartz. The heavy mineral fraction contains translucent olive-green pyroxene and hornblende, euhedral dark grains of spinel, and mostly fragmented garnet with subordinate euhedral grains. Zircon, rutile and tourmaline are rare implying an immature character of the sediment (Hubert, 1962).

Sample IK8-1 from the Keramaian Formation is a medium sorted, grain supported siltstone with some sand-sized components. The intergranular space is filled with clay minerals and calcite. Fragments are predominantly monomineralic and of angular to sub-angular shape, consisting of monocrystalline quartz, plagioclase, hornblende, diopside, muscovite, and brownish-translucent Cr-spinel with minor glaucophane, kyanite and rounded glauconite. Lithoclasts are predominantly muscovite–sillimanite-bearing quartzites.

Sample IK9-1 from the Keramaian Formation is an andesitic litharenitic sandstone grain with minor interstitial chlorite and angular volcanic fragments, which sometimes show signs of propylitic alteration by breakdown of primary minerals to epidote and muscovite.

The Manunggul Formation sample M3 is a semi-consolidated conglomerate that has not been described petrographically. Macroscopically, the sample consisted predominantly of well-rounded volcanic and minor (meta-)sedimentary (e.g. quartzites and mica schists) lithoclasts. The moderately-sorted limonitic sandstone IK22-8 (Manunggul Formation) contains predominantly angular to subangular quartz clasts of metamorphic (with mica) and magmatic origin. The minor lithic constituents are radiolarites and elongated, deformed claystones and psammites. Zircon, rutile, tourmaline, garnet and apatite are fairly common and appear concentrated.

Sample IK21-1 represents volcaniclastics of the Paau Formation (Upper Pitanak Group). The sample is a moderately sorted, clast-supported sandstone, in which the intergranular space is filled with silt or clay-material. The clasts are predominantly angular monomineralic fragments (plagioclase, K-feldspar, and hornblende). The heavy mineral fraction is dominated by euhedral to subhedral apatite, hornblende, pyroxenes, and opaques. Zircon is rare and always euhedral in shape. Subaerial deposition can be inferred by the presence of fossilized mudcracks present at the outcrop.

3.2. Zircon ages

An overview of the zircon age distributions can be found in Fig. 3 and Table 1 in the Electronic Appendix 2 provides a summary of the sedimentary samples, including the three youngest analyzed zircon ages. The observed U–Pb ages for zircons range from the Neoarchean to the Late Cretaceous (3166 to 76 Ma). The Cempaka Quaternary sands ($n = 92$) yield two distinct Mesozoic age peaks between 79 to 104 Ma and 127 to 169 Ma, a small population of Carboniferous zircons 303 to

Please cite this article as: Kueter, N., et al., Tracing the depositional history of Kalimantan diamonds by zircon provenance and diamond morphology studies, Lithos (2016), http://dx.doi.org/10.1016/j.lithos.2016.05.003

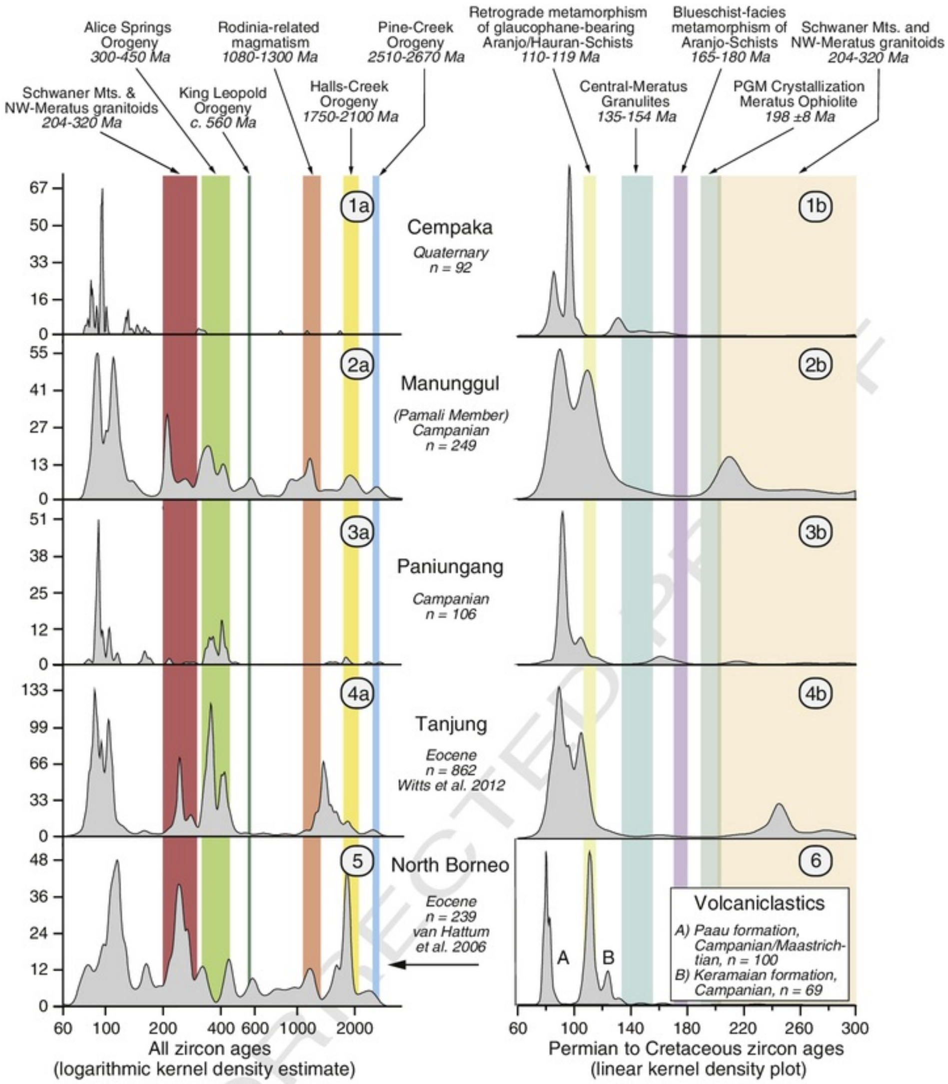

Fig. 3. Zircon provenance Zircon age distribution in our samples (nos. 1–3, 6) and literature data from Witts et al. (2012) for the unconformably overlying Eocene Tanjung Formation (no. 4) and from van Hattum et al. (2006) for the North Borneo Eocene turbidites of the Crocker Formation (no. 5). Recognizable in all samples is the late Cretaceous igneous activity. Note that the zircon distributions of two Meratus volcaniclastic sediments (no. 6, A and B) match with the two Cretaceous ages peaks observed in the other samples. Zircon age densities corresponding to the age of the Central Australian Alice Springs Orogeny are visible in 2a, 3a, and 4a. The Manunggul Formation (no. 2a) and the Crocker Formation of North Borneo (no. 5) have a comparable age spectrum and display as only samples an age peak corresponding to the Northwestern Australian King Leopold Orogeny. A prominent age density around 1400 Ma is restricted to the Eocene Tanjung Formation (no. 4a). A logarithmic display of kernel density estimates (left side) minimizes age intervals of no information. The 60 to 300 Ma close-up displays a linear kernel density estimate. Plots were made using the *DensityPlotter* program of Vermeesch (2012). The same color code is used in Fig. 10.

331 Ma, and three Precambrian zircons of 821.7 ± 5.5 Ma, 1128 ± 7.6 Ma and 1675 ± 12 Ma ages.

The zircon age distributions of both the Manunggul samples (M3, IK22-8) appear very similar and are therefore combined in Fig. 3. The zircon ages in these samples range from 80 to 3166 Ma. Late Jurassic to Cretaceous zircons make c. 40% of the populations, a smaller number of zircons yield Permian to Early Jurassic ages, and Silurian to Carboniferous ages. An almost homogenous distribution of zircon ages is observed between the Early Paleozoic to the Neoarchean with some less-pronounced age densities.

The Paniungang Formation (IK20-1) contains predominantly Cretaceous zircons crystallized between 80 and 160 Ma, two populations of Silurian to Carboniferous and Triassic to Jurassic zircons, and six zircons of Proterozoic age. The observed ages range from 81 to 2704 Ma.

The volcaniclastic samples of the Keramaian (IK9-1) and Paau formations (IK21-1) yield distinct Cretaceous age densities: the age interval of the Keramaian sample ranges from 102 to 163 Ma with a mode at 112 Ma. The Keramaian Formation sample IK8-1 did not provide enough zircons for a provenance analysis. The Paau sample yields upper Cretaceous zircon ages between 76 and 92 Ma with a mode at 81 Ma, with the exception of a single grain of 230 ± 5.4 Ma age.

3.3. Zircon shape, color and age correlation

Dated zircons from the Paniungang Formation (IK20-1), Manunggul Formation (IK22-8 and M3), and the Cempaka Pleistocene paleo river channel were classified following Witts et al. (2012) into the following: class 1—non-abraded crystals, class 2—abraded crystals with rounded ends but remaining primary faces, and class 3—profoundly abraded or rounded crystals. A correlation between age and abrasion is observed (Fig. 4) as an age-progressive trend toward strongly abraded crystals, with non-abraded crystals dominating among the younger grains.

A notable feature in the Cretaceous sediments are strongly abraded spherical pinkish or brownish colored zircons (cf. Electronic Appendix 2) comprising up to 3% of all recovered zircons. This finding is in good agreement with observations of Witts et al. (2012) who report 3.6% colored zircons in the Eocene sediments. In this study, the pink zircons are older than Early Carboniferous (youngest pink zircon 354 ± 4.5 Ma) and the two brown zircons date at 90.2 ± 1.2 and 278 ± 3.5 Ma. The oldest colored zircon is a pink grain from the Manunggul Formation with an age of 2509 ± 19 Ma. The age distribution of both pink and brown zircons appears homogeneous with no apparent age densities.

3.4. Zircon trace element chemistry

Belousova et al. (2002) proposed to discriminate the provenance of detrital zircons based on their trace element chemistry. Here, we use the "short" CART-tree discrimination scheme from Belousova et al. (2002), which provides an 80% probability of correct zircon classification for carbonatitic and 88% for kimberlitic sources. The zircons identified as different to "kimberlitic" or "carbonatitic" are labeled as "crustal" due to the limitations in discrimination among crustal zircon sources (e.g. Hoskin and Ireland, 2000). In our dataset of 1393 detrital zircons analyses, 120 crystals were identified by CART as either "kimberlitic" ($n = 10$) or "carbonatitic" ($n = 110$).

Using literature data for kimberlitic and peridotitic zircons worldwide (Belousova et al., 1998; Belousova et al., 2002; Page et al., 2007; Zheng et al., 2006), we further reduced this subset of analyses by applying quality criteria based on the maxima and minima of the published values: P < 110 ppm, Y < 981 ppm, Th < 50 ppm, U < 170 ppm, Th/U < 0.85, $Ce/Ce_n > 0.84$ and $Eu/Eu_n > 0.23$ (with Ce_n and Eu_n C1-normalized after (McDonough and Sun, 1995); Cf. electronic appendix 2).

This second data reduction dismissed all zircons previously assigned to kimberlitic sources due to low Th/U-ratios, elevated U contents or distinct negative Eu-anomalies. Thus, only 51 zircons still show an affinity to carbonatites, of which 80% belong to the macro-sized zircon fraction (>355 μm) of the Pleistocene paleo river. The rare earth element (REE) patterns of carbonatitic zircons are similar to crustal zircons but show lower REE-concentrations (36 to 254 ppm, average 122 ppm) and are nearly devoid of negative Eu-anomalies (Fig. 5A).

The U–Pb age dating on this subset of carbonatitic and kimberlitic zircons resulted in 38 concordant ages mainly covering a Mesozoic crystallization interval between 134 and 174 Ma. Six kimberlitic zircons fell outside this interval yielding ages of 102 to 108 Ma and 314 ± 15 Ma.

3.5. Garnet provenance analyses

The variable chemical composition of garnet makes it an important mineral for both sediment provenance studies and for kimberlite exploration. An Excel spreadsheet by Locock (2008) was used for the mineralogical classification of the 767 garnet analyses. The dataset was further screened for mantle-garnets using the empirical classification schemes from Schulze (2003) and Grütter et al. (2004), returning no peridotitic or kimberlitic (macrocrystic-) garnets. The chemical compositions of 141 garnets fall into the fields of group II (Schulze, 2003) and G3- and G4-garnets (Grütter et al., 2004) corresponding to pyroxenites and eclogites. However, none of these grains indicate a deep mantle origin or diamond association because the critical concentration of $Na_2O > 0.07$ wt.% typical for a deep mantle garnet was not detected (see Electronic Appendix 1, data table "garnets").

On the discrimination diagram for mantle and crustal garnets ((Ca / (Ca + Mg) vs. Mg / (Mg + Fe_t); Schulze, 2003) the majority of the garnet analyses overlap the delineation line between the two fields

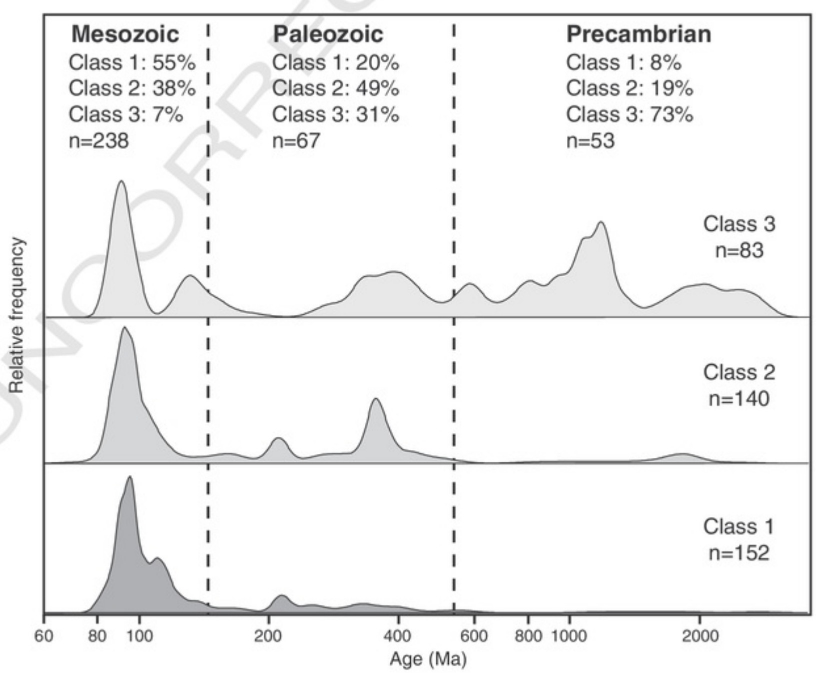

Fig. 4. Zircon abrasion Logarithmic kernel density plot (Vermeesch, 2012) of zircons with varying degree of abrasion. Non-abraded zircons of class 1 dominate in the Mesozoic. Half of the zircons in the Paleozoic yield moderate (e.g. broken apexes, corrosion pits but remaining crystal faces) abrasion inferring prolonged alluvial transport. Precambrian zircons are predominantly heavily abraded crystals (74% class 3), often brown or pink in color. Such zircons presumably experienced extended alluvial transport and multiple erosional cycles.

Please cite this article as: Kueter, N., et al., Tracing the depositional history of Kalimantan diamonds by zircon provenance and diamond morphology studies, Lithos (2016), http://dx.doi.org/10.1016/j.lithos.2016.05.003

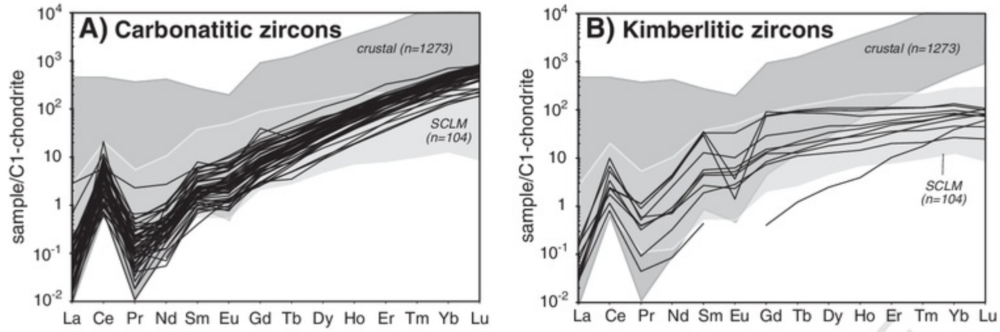

Fig. 5. Zircon REE Spider plot of C1-normalized (McDonough and Sun, 1995) REE-contents in zircon. The "SCLM" field comprises of >99% analyses of kimberlite- and peridotite-hosted zircons described by Belousova et al. (1998), Page et al. (2007) and Zheng et al. (2006). The "crustal" field are all zircons identified other than "kimberlitic" or "carbonatitic" by the "short" CART-tree of Belousova et al. (2002). Shown are the REE-pattern of 51 zircons with carbonatitic affinity and 10 zircons of kimberlitic affinity (cf. Section 3.4). Carbonatitic zircons are relatively depleted in REE and coincide well with the SCLM-zircon literature-values for LREE. However, they show a steep slope in the HREE, similar to the majority of crustal zircon. Zircons with kimberlite affinity are low in REE-concentration and feature a strong garnet signal as displayed by the flat HREE-tail. The REE-pattern generally overlies well the sometimes be observed to small degrees in zircons from eclogites (e.g. Rubatto, 2002).

with only two garnets from the Manunggul Formation falling well inside the mantle-array (Fig. 6).

On the ternary scheme proposed by Mange and Morton (2007) to assess the growth environment of detrital garnets (Fig. 7), the Paniungang Formation garnets ($n = 225$; IK20-1) form clusters in the fields of intermediate to acidic igneous rocks and amphibolite-facies metasedimentary rocks. They are predominantly Ca and Mg-enriched almandines. Almost 8% of the Paniungang garnets show an affinity to amphibolite facies metasediments and high-grade metabasic rocks.

Garnets ($n = 131$) from the Keramaian Formation (IK8-1) are predominantly almandines and Fe-enriched grossulars that can be assigned to amphibolite-facies metasedimentary lithologies. A minor population (7%) yield affinities to amphibolite facies metasediments and high-grade metabasic rocks. Those grains were also identified as G3 and G4 garnets, respectively. Few grains intercept with the field for peridotitic garnets (Fig. 7).

The garnet data from the two Manunggul sandstone samples was combined (IK22-8 & M3) into a single group of 287 grains due to their similar composition. They cover all classification fields. The majority of garnets can be assigned to amphibolite facies metasediments and high-grade metabasic rocks. Mg-enriched almandines are more abundant than in other garnet populations and some overlap with the fields for high-grade metabasics rocks, pyroxenites, and peridotites. The majority of these high-Mg grains correspond to an eclogitic source: c. 27% according to Schulze's (2003) classification and c. 16% according to Grütter et al.'s (2004) classification.

Garnets from the Cempaka Quaternary alluvium ($n = 124$) are mainly almandines and spessartines with a uniform composition missing any compositions similar to eclogitic, peridotitic, or kimberlitic garnets. Mn-rich spessartines plot within the compositional fields of Type II, G3 and G4 on diagrams from Schulze (2003) and Grütter et al. (2004) (Fig. 6). However, all these garnets contain more than 2.8 wt.% MnO and thus exceed the maximum value of MnO for mantle-derived garnets (Grütter et al., 2004).

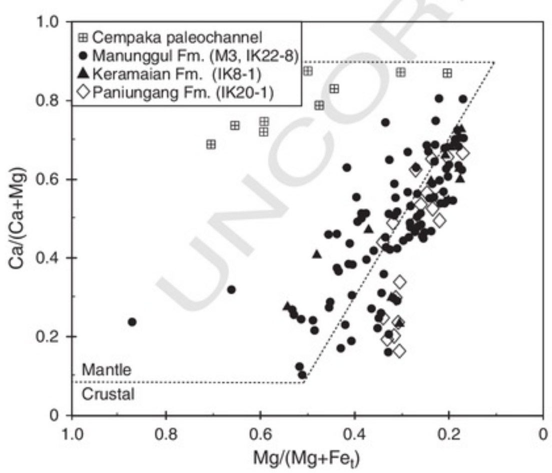

Fig. 6. Garnet_A Classified as eclogitic and pyroxenitic G3 and G4 detrital garnets plotted in the mantle–crust discrimination diagram of Schulze (2003). The G-garnets roughly follow the demarcation line and only few grains plot within the mantle-field. Note that the Cempaka garnets (crossed square-symbols) which plot within the mantle-field are actually Manganese-rich grossulars. These garnets are falsely identified as mantle-derived (cf. Section 3.5).

3.6. Glaucophane

The sample from the Keramaian Formation contained blue amphibole, which was identified as glaucophane and glaucophane-variety crossite (Tindle and Webb, 1994). Their chemical composition is similar to crossite relicts reported from retrograde amphibolite-facies schist from the Aranjo/Hauran-metamorphites in the central Meratus (Soesilo, 2012; cf. Electronic Appendices 1 and 2). Glaucophane is a good provenance indicator of the exhumation and erosion of a blueschist-bearing metamorphic terrane (Mange and Morton, 2007; Winkler and Bernoulli, 1986). This finding is in good agreement with the aforementioned presence of eclogitic garnet.

4. Results—Diamonds

We examined the morphology, color, surface dissolution and abrasion features on 247 diamonds from Southeast Kalimantan (KS) and 85 diamonds from West Kalimantan (KB). Unless indicated differently, all percentages in the following text are given in reference to all stones within either the KS or the KB suite. The KB suite has larger stones with in average mean weight of 0.012 g compared to 0.005 g in the KS suite. This may affect comparison of the erosional surface wear since larger diamonds are more prone to gain fractures and scars. A complete list of diamond samples is provided in the electronic appendix 1 and an overview of the results discussed in the following can be found in Table 4 in the Electronic Appendix 2.

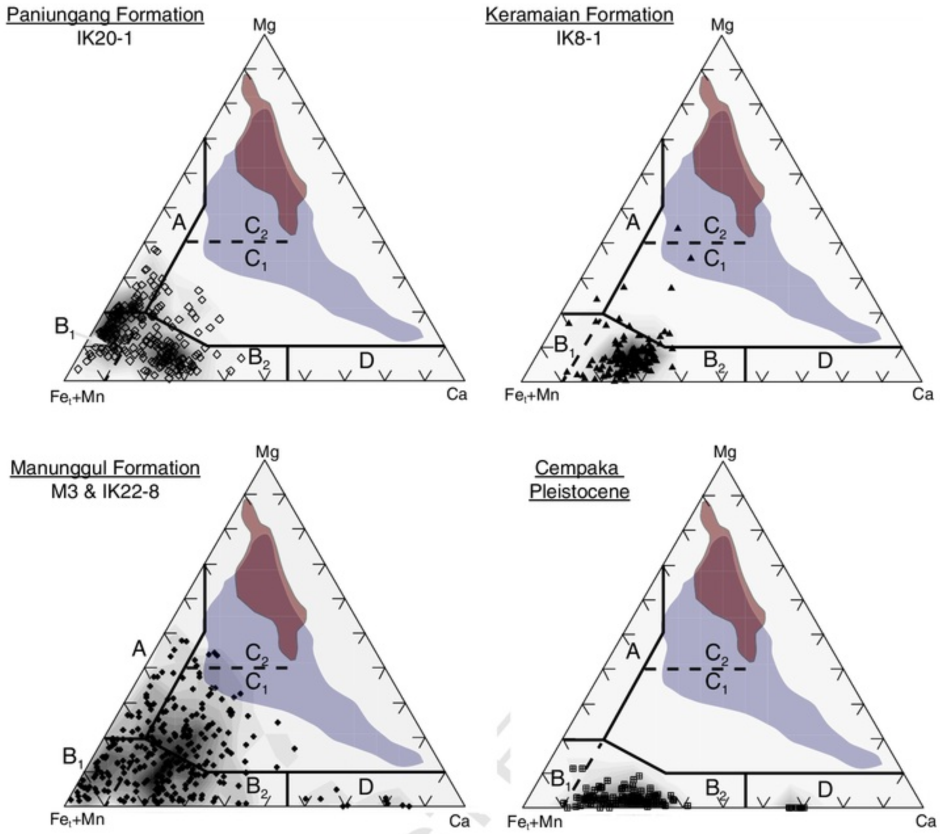

Fig. 7. Garnet_B Triangular provenance plot for detrital garnets after Mange and Morton, 2007. Garnets of letter-labeled fields are mainly derived from: A = high-grade granulite-facies metasediments or charnokites, B_1 = intermediate-acidic igneous rocks, B_2 = amphibolite-facies metasediments, C_1 = high-grade metabasics rocks, C_2 = ultramafic rocks, D = low-grade metabasics rocks, skarns, and calc-silicate granulites. Colored fields show the distribution of kimberlitic (red) and peridotitic (blue) garnets from the dataset of Grütter et al. (2004). Only few garnets plot within the blue peridotite field. Paniungang garnets yield two densities in the amphibolite-facies field B, Keramaian and Cempaka garnets are restricted to field B_2. Uniformity distributed appear detrital garnets from the Manunggul formation, with a slightly pronounced abundance of grains with metabasics and ultramafic affinity (C_1 & C_2). These grains are also identified as eclogitic G3 and pyroxenitic G4 garnets by the Grütter et al. (2004) classification.

4.1. Morphology

Octahedra with variable degree of resorption are slightly more abundant among the KS diamonds, whereas tetrahexahedral diamonds (THH) make up c. 45% of the KB diamonds and only c. 26% of KS diamonds. Cubo-octahedrons, pseudohemimorphic and aggregate diamonds appear in similar proportions in both deposits, and dodecahedral diamonds are slightly more abundant in KS. The amount of aggregates (Fig. 9A) and complex shaped diamonds (serrated and fractured; e.g. Figs. 8F and 9E) is higher in KS. Brown or (canary-) yellow cubo-octahedrons form a distinct type in both suites. Their {100}-faces are densely covered with point-bottomed square-pits and the remaining facets are coarsely striated. Smith et al. (2009) also reported colorless cubo-octahedrons (e.g. Fig. 2D in their publication), very similar to our specimen shown in Fig. 8H. The "diver's helmet"-shape diamonds as described by Smith et al. (2009) were recognized in Kalimantan Barat (not sampled) and is represented by a single colorless stone in the KS-suite. The KS suite contains one fibrous cube and one coated stone ("Balla"). Coated stones are occasionally reported from Kalimantan Selatan (Spencer et al., 1988), for example the 2008 discovered 200 ct "Putri Malu" that was found in central Meratus (Antaroku village, Banjar District).

The degree of resorption was determined using the resorption morphology scheme of McCallum et al. (1991) originally developed for diamonds that resorb into a THH shape, but was also applied for dodecahedral diamonds in this study. Fully resorbed diamonds (class 1) and diamonds with resorption exceeding 75% (classes 2 and 3) dominate in both localities. The crystals are predominantly THH (27% in KS to 45% in KS) but 16%–18% of the secondary habits are dodecahedra. Classes 1 and 2 stones show a glossy appearance preserved on 19%–22% of diamonds from KS and KB, respectively (Fig. 9B). Octahedral diamonds with minor resorption (classes 4 to 5, 12% in KB and 20% in KS) commonly feature di-trigonal shapes of their {111}-faces (Fig. 8B), while trigonal {111}-faces (Fig. 8A) are less abundant. Non-resorbed diamonds are rare (<1%).

4.2. Color and deformation

All diamonds were grouped as colorless, brown, yellow or "other color"; the latter group includes stones with radiation-induced greenish and brownish overtones. KS and KB populations show significant differences in the proportions of colorless and brown stones but similar amounts of yellow stones (14% in KB to 17% in KS). Colorless stones are four times more abundant in KS (40%) than in KB (c. 9%) and brown stones make up 62% in KB and only 38% in KS. A single pale-pink octahedral diamond was recognized in the KS suite (Fig. 8F). Rare but regular findings of pink diamonds were also reported by PT-Galuh Cempaka (pers. comm. Kuncoro Hadi and Bob Nugroho, PT-Galuh Cempaka; cf. Supplementary material). Deformation lamellae are present on 40% and 27% of KB and KS diamonds, respectively (Fig. 9D). 75%

Please cite this article as: Kueter, N., et al., Tracing the depositional history of Kalimantan diamonds by zircon provenance and diamond morphology studies, Lithos (2016), http://dx.doi.org/10.1016/j.lithos.2016.05.003

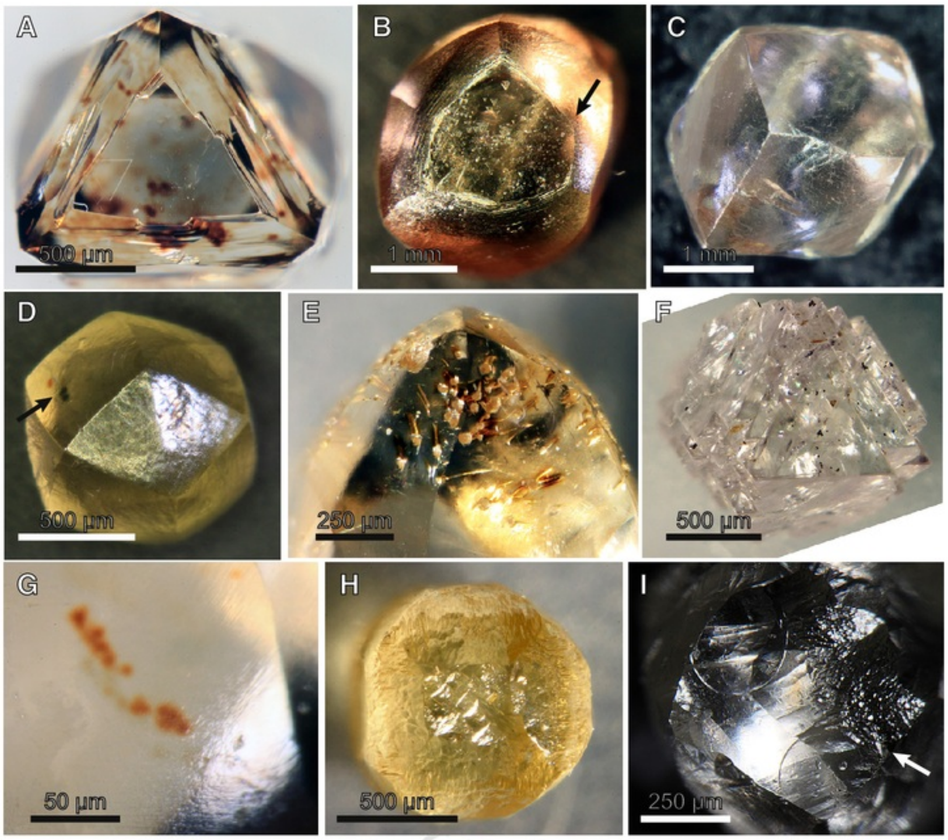

Fig. 8. Diamonds Some representative diamond samples: A) A colorless, strongly resorbed class 4 octahedron with flat-bottomed triangular etch pits on the (111) face and plenty brown radiation spots. The resorbed edges of the {111} faces proceed straight. B) Brown-colored Octahedra-THH transition form (Class 3). The resorbed surfaces yield a fine frosting. The remaining {111} faces show a kink imposing a di-trigonal outline (arrow) and plenty of tiny flat-bottomed trigonal etch pits. C) A colorless dodecahedral diamond (class 1) with abrasion scars on its surface (tiny cleaved, network pattern). D) Yellow THH diamond (class 1) with a finely frosted surface and a brown and green radiation spot (arrow). E) Glossy brown THH with deep hexagonal etching. All channels reach the diamond surface and are often surrounded by a brownish, likely radiogenic halo. F) Pale pink octahedral diamond (class 6) with straight edges and multiple apexes. This stone shows only minor abrasion. G) Trail of brown radiation spots on a finely frosted THH-surface. H) Canary-yellow cubo-octahedron with point-bottomed square-pits on the {100} faces and coarsely-striated {110} faces. I) Two circular etch pits on a finely frosted THH stone. The upper rim of the lower disk is overprinted by a coarsely-frosted island (arrow).

of the diamonds with deformation lamellae have a brown color. Radiation spots are present on 28% of KS and 47% of KB diamonds. Green radiation spots are rare (2% in KS and 6% in KB), while brown spots are dominant (26% in KS and 41% in KB; Fig. 8A, D and G).

4.3. Etch features

Etch features are present on 21% of the diamonds from KS and 33% from KB; we note that the proportion could be affected by the difference in the average stone size (Fedortchouk et al., 2005). Diamonds with preserved {111}-faces show flat-bottomed trigons (Fig. 8A) more commonly in KS (37%) than in KB (24%), while point-bottomed trigons predominate in KB (48% vs. 19% in KS; Fig. 8B). Hexagonal etch pits were almost exclusively observed in the KB-suite (14% of all stones), while only one KS diamond yields hexagonal etch pitting on a chemically corroded cleavage plane (Fig. 9E). KB contains also two diamonds with deep etch channels with a hexagonal outline. These needle-like pits are surrounded by a brownish halo likely of radiogenic origin (Fig. 8E). In both suites, c. 17% of diamonds yield circular elevations and depressions (disks; Fig. 8I).

More than half of the diamonds in both suites yield signs of frosting on their resorbed surfaces (e.g. discrete islands with relatively rough surface). Profound frosting that affects all faces or covers the diamond entirely is present on 48% of the KB diamonds and 37% of the KS diamonds (Fig. 8D). Some dodecahedral diamonds show coarse frosting or an edgy skin similar to the products of diamond-graphitization experiments (Davies and Evans, 1972; Fedortchouk et al., 2007)(Figs. 8I and 9C). Few chipped diamonds have frosted surfaces on the cleavage planes (Fig. 9E and F).

4.4. Abrasion features

We examined the presence of the abrasion features on all faces of each diamond under a stereoscope at a fixed magnification of 50× using the description-scheme (Table 2 in the electronic appendix 2). Abrasion features such as "network patterns" and percussion marks are more common on KB diamonds (45%) compared to KS diamonds (14%), possibly due to the larger average stone size in the KB population. Fig. 3 in Smith et al. (2009) shows "rhombic abrasion" on only c. 5% in KS and c. 30% in KB diamonds. 45% of the KS diamonds yield no apparent abrasion.

4.5. Mineral inclusions in diamonds and thermo-elastic barometry

Four diamonds were found suitable for in-situ X-ray diffraction investigation of their mineral inclusions. Diamonds CEM 152, CEM 161,

Please cite this article as: Kueter, N., et al., Tracing the depositional history of Kalimantan diamonds by zircon provenance and diamond morphology studies, Lithos (2016), http://dx.doi.org/10.1016/j.lithos.2016.05.003

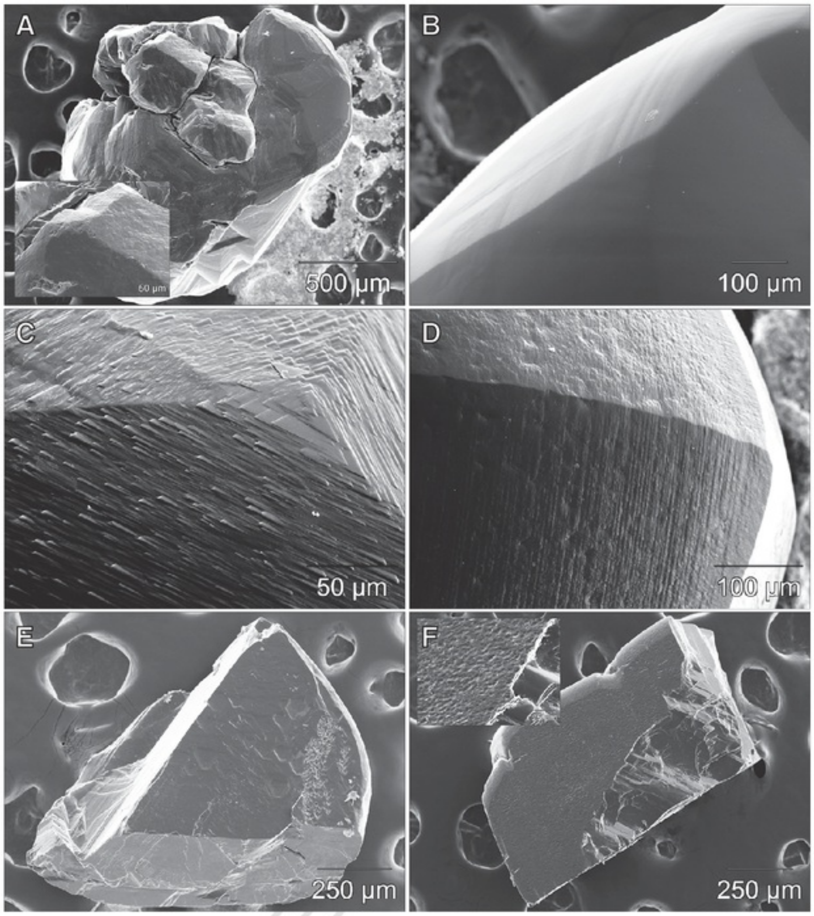

Fig. 9. Diamond SEM SEM-images of Kalimantan Selatan diamond crystals. A) Aggregate from Kalimantan Selatan showing slight resorption preserving di-trigonal {111} faces. The aggregate shows cracks along the crystal-interfaces and some edge-abrasion. B) Smooth, almost feature-less surface of a THH-crystal with glossy surface. C) Dodecahedron with coarse frosting (few tens of microns large) probably resulted from graphitization within a volatile-undersaturated melt. {111} faces form edgy triangular features. D) Finely frosted THH-crystal with deformation lamellae with micron-sized frosting only. E) Chipped diamond with flat-bottomed hexagonal and trail of point-bottomed trigonal etch pits on fracture face 1 probably created and resorbed during volcanic emplacement. Absence of chemical corrosion features on fractured faces 2 and 3 indicating post-eruptive genesis. F) Chipped diamond with finely frosted surface that was later fractured. Close-up: Boundary between chemically corroded surface on the left side and a postdating (lowered) physical fracture on the right side.

CEM 61 and KB 52 showed in total at least six optically visible mineral inclusions.

Diamond CEM 152 contains three separated inclusions of olivine with their largest diameters: about 0.2 mm, about 0.1 mm, and c. 0.05 mm. The equations of state for Mg-rich olivines (Nestola et al., 2011b) using their chemical composition (Table 5 in the Electronic Appendix) confined the residual pressure between 0.14 and 0.18 GPa.

The same result we obtained for olivine inclusion in diamond KB 52. Olivine inclusions trapped in diamonds and showing no fractures give the residual pressure of 0.4 to 0.7 GPa (Nestola et al., 2011a). As described in (Angel et al., 2014a,b, 2015a,b) and Nestola et al. (2011a), it is possible to obtain the pressure of entrapment from these residual pressures, i.e. pressure of formation of the diamond-inclusion pair. This is based on the assumption that no anelastic phenomena developed at the inclusion-diamond interface during the ascent of diamond to the Earth's surface, such as fractures precluding the calculation of reliable pressure of formation. We interpret our unusually low residual pressure results to be due to microscale fractures, thus our present results on olivine cannot be used to derive reliable values for the pressure of formation.

A coesite inclusion in diamond CEM 61 shows a very high residual pressure, larger than 2 GPa. However, Howell et al. (2012) demonstrated that coesite presently do not allow the determination of reliable values for the pressure of formation and cannot be used as a reliable geobarometer. For example, the calculated pressure of formation of 2.94 GPa for our coesite at a fixed temperature of 1000 °C is unrealistically low compared to the minimum pressure of 4 GPa at 1000 °C required to reach the diamond stability field. The reason why coesite does not seem to be a good geobarometer may be related to its thermal expansion which appears to be similar to that of diamond, based on the available data in literature (Howell et al., 2012).

The most important result of our X-ray investigation is provided by an inclusion of peridotitic garnet (cf. Electronic Appendix 2). From the composition retrieved via crystal structure refinement, a unit-cell volume equal to 1541.13 Å^3 at room pressure can be calculated by using data from Milani et al. (2015) and Dymshits et al. (2014). The unit-cell volume measured on our garnet trapped in diamond CEM 161 is 1538.24 Å^3, corresponding to a volume difference of 2.89 Å^3 between the calculated value at room pressure and the value determined within the diamond host. According to the pressure–volume equations of state

Please cite this article as: Kueter, N., et al., Tracing the depositional history of Kalimantan diamonds by zircon provenance and diamond morphology studies, Lithos (2016), http://dx.doi.org/10.1016/j.lithos.2016.05.003

published in Milani et al. (2015), such a volume difference results in an internal pressure equal to 0.35(2) GPa. When applying the elastic geobarometry described in Angel et al. (2014b) and Angel et al. (2015b) on this value and by using the software EOSFIT7.C (Angel et al., 2014a), we obtain a pressure of formation between 4.83 and 6.04 for fixed values of temperature of 930 and 1250 °C, respectively. The employed temperature estimates for the Kalimantan diamonds are based on Smith et al. (2009) who estimated pressures of formation between 4.2 and 4.4 GPa based on the Cr-in-garnet geobarometer. However, Smith et al. (2009) state that if the Cr-spinels and subcalcic garnet represent co-existing populations then for a temperature of 1100 °C they could estimate a pressure of about 6 GPa, this value being much closer to our pressure determination.

5. Discussion—Sediments

5.1. Zircon age provenance

Zircon age densities obtained from all samples imply a continuous zircon production between the Mid Jurassic and Late Cretaceous (Fig. 3). A similar continuum of zircon ages is present in the large dataset for the Eocene Tanjung Formation of Witts et al. (2012); Fig. 3-4B). This age interval reflects both igneous activity during the Meratus orogeny and the onset of calc-alkaline magmatism. Clements et al. (2011) and Witts et al. (2012) suggest the Schwaner Mountains in South-Central Borneo as a source for Cretaceous zircons. However, a more proximal zircon source within the rising Meratus is favored because Cretaceous zircons in all clastic sediments correlate well with the zircon age intervals of two volcaniclastic sediments of the Keramaian Formation (IK9-1) and the Paau Formation (IK21-1; Fig. 3-6). Deposited close to their primary source within the Meratus orogen, these immature volcanic sediments likely acted as an important sediment supplier for later clastic sediments. The respective samples show age modes at c. 80 Ma and c. 110 Ma that are also visible in the other age spectra in Fig. 3, thus referring to two main magmatic episodes. Numerous Barremian to Early Campanian zircon ages correlate with calc-alkaline intrusions that penetrated the Meratus basement ((Soesilo, 2012; Yuwono et al., 1988); Kueter, unpublished). The 110 Ma mode also overlaps with K–Ar ages for greenschist–retrograde Aranjo/Hauran schist (alternative names in use; Fig. 2) (Parkinson et al., 1998; Wakita et al., 1998).

Jurassic to Early Cretaceous ages coincide with the onset of orogenic magmatic activity during terrane accretion. The ages of detrital zircons agree with a 154 to 135 Ma U–Pb age interval of zircons from Meratus garnet-granulites (Soesilo, 2012). Haile et al. (1977) also reported 155 Ma K–Ar ages from the Schwaner Mountain granitoids. Few Early Jurassic zircon ages overlap with two K–Ar ages of 180 and 165 Ma obtained from the glaucophane-bearing Aranjo/Hauran schist. Soesilo (2012) interprets these schists as showing "remnant ages" of incompletely retrograded blueschists formed prior to the collision of the EJT with the SWB (Fig. 1). Permian and Triassic zircons are recognized from Eocene sandstones of the Crocker Formation (NE-Borneo, Fig. 3-5) and the Eocene to Miocene clastic sediments in the Meratus area (Fig. 3-4a) and are commonly assigned to the tin-belt granitoids of the Malay Peninsula (Hall and Sevastjanova, 2012; Sevastjanova et al., 2011; van Hattum et al., 2006). However, many of our zircons show only minor abrasion, thus we favor a proximal source such as the 320–204 Ma (K–Ar) granitoids from the Schwaner Mountains reported in Williams et al. (1988) or the 319 and 260 Ma (K–Ar) granites in the northwestern Meratus reported in Dirk and Amiruddin (2000). Furthermore, Witts et al. (2012) proposes sources located in the Karimunjawa Arch (Fig. 1).

All our samples contain Silurian to Carboniferous zircon populations and are especially abundant in the Paniungang and Manunggul formations as well as in the unconformably overlying Eocene Tanjung Formation as reported by Witts et al. (2012). These and older zircons predate both the collision between the EJT and SWB, as well as the formation of the oceanic lithosphere that comprises the Meratus ophiolite. The first breakup of the continental blocks (including West Sumatra and East Malaya blocks proximal to Kalimantan; Fig. 1) from Australian–Gondwanaland is constrained to the Carboniferous (Metcalfe, 2011). Accordingly, such zircons must be derived from sources pre-dating the rifting. Their prolonged alluvial history can be inferred by the dominance of abraded class 2 and strongly abraded class 3 zircons (Fig. 4). Debris from the intracontinental 450 to 300 Ma Alice Springs orogeny in central Australia (Fig. 11) accumulated in sedimentary basins of the North Australian Craton, for example the Canning Basin (Buick et al., 2008; Haines et al., 2001). These basins could be a potential source for the Silurian to Carboniferous zircons. With respect to the diamond part of this paper, it is worth mentioning that the emplacement of the adjacent Merlin kimberlite field (376 ± 4 Ma via (U–Th–Pb)/He on zircon; McInnes et al., 2009) coincides with the peak of the Alice Springs orogeny (Haines et al., 2001) (Fig.11).

All our samples contain Cambrian, Proterozoic and Neoarchean zircons as also described for northern Borneo, Java and Karimunjawa in previous works (Sevastjanova et al., 2011; Smyth et al., 2007; van Hattum et al., 2006; Witts et al., 2012). A small cluster of c. 580 Ma zircons is solely recognized in the Manunggul Formation samples (Fig. 3.2a) and from the Eocene Crocker Formation in North Borneo (Fig. 3.5, van Hattum et al., 2006) and could correspond to the age of the King Leopold orogeny (Tyler and Griffin, 1990; Tyler et al., 2012)(Fig. 10). However, no reports for synchronous zircon-forming events were found in the literature.

Paleo- to Mesoproterozoic zircon ages coincide with the timing of magmatic events during the amalgamation of the Rodinia supercontinent at around 1300 Ma. Rodinia remnants are present in Western Central Australia, such as the 1300 Ma Rundall granite, 1200–1150 Ma Musgravian metamorphic assemblage and 1190–1150 Ma granites, the 1080 Ma Tollu volcanics and gabbroic/granitic intrusions of the Giles Complex (Myers et al. (1996) and references therein) (Fig. 10).

Age densities between 2100 to 1750 Ma could be linked to Paleoproterozoic granitoids of the King Leopold and Halls Creek fold belts framing the Kimberley region (Tyler et al. (2012) and references therein, Fig. 10). A small population of six Neoarchean zircons (2704 ± 26 to 2509 ± 19) fit with zircon crystallization ages of 2670 to 2510 Ma from the North-Australian Pine Creek orogen (Hollis et al., 2009). Isolated Paleoproterozoic and Neoarchean zircon grains that are not assigned to specific sources still point towards a cratonic origin. The strongly abraded appearances of Precambrian zircons (19% of class 2 and 73% of class 3; Fig. 4) may be linked to multiple sedimentary cycles through the Earth's history. The presence of a small number of non-abraded Precambrian zircons may indicate limited alluvial transport, inferring a long-term storage in Precambrian host rocks and late liberation by erosion.

5.2. Depositional constraints on Cretaceous sediments

The youngest concordant age of detrital zircon in a sediment confines its earliest possible time of deposition (Fedo et al., 2003). Therefore, depositional times for all clastic sediments are the Campanian and Maastrichtian, which is in agreement with previous age constraints (Hashimoto and Koike, 1973; Sikumbang, 1986; Sikumbang and Heryanto, 1994). An exception is the Paniungang Formation, whose youngest detrital zircon age of 81.4 ± 1.6 Ma is roughly 15 myr younger than the youngest deposition age of the Upper Coniacian as depicted in the geological map of by Sikumbang and Heryanto (1994).

The main detrital source is calc-alkaline plutonic and volcanic rocks. Sedimentary lithoclasts (clays and sandstones marls) indicate derivation of detrital material from older sedimentary strata. Reworked sediments are generally indicated by the presence of monocrystalline quartz, clay-, silt-, and sandstone lithoclasts, rounded heavy minerals

Please cite this article as: Kueter, N., et al., Tracing the depositional history of Kalimantan diamonds by zircon provenance and diamond morphology studies, Lithos (2016), http://dx.doi.org/10.1016/j.lithos.2016.05.003

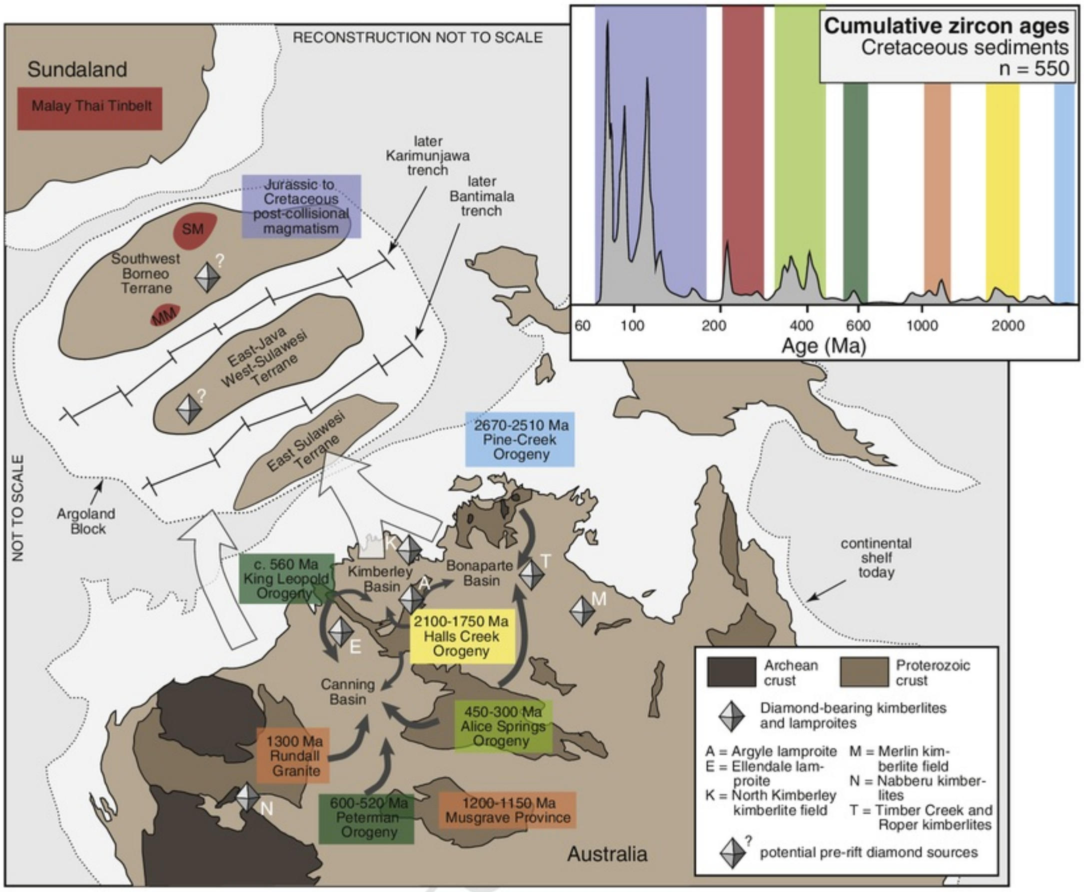

Fig. 10. Summary Schematic illustration highlighting potential primary zircon provenances in Northwestern and Central Australia. Diamond symbols with assigned letters represent known diamond-bearing kimberlite and lamproite provinces in Northwestern Australia. The top-right graphic is a cumulative age density plot of zircons from Cretaceous sediments analyzed in this study. The color coding corresponds to the orogenic provinces shown in the map and is the same as in Fig. 3. These provinces shed sedimentary material, including diamonds and zircons, into the surrounding big sedimentary basins (e.g. Canning or Kimberley basin; black arrows). These basins might have extended to the north where later lithospheric fragments detached. Diamond-bearing basin lithologies and possibly also primary diamond sources (indicated by diamond-symbols with question marks) drifted northwards forming the present-day continental core of Southeast Asia. Terrane accretion-related orogenic events could have metamorphosed wide parts of diamond-bearing lithologies resulting in the destruction of diamond-indicator minerals but also led to the re-liberation of diamonds from exhumed host rocks. Abbreviations: SM = Permo-Triassic Granitoids of the Schwaner Mountains; MM = Permo-Triassic granites from the North Meratus (cf. Section 5.1).

including pre-Permian zircons, tourmalines and rutiles. Pre-collisional, allochthonous sediments have not been described in the Meratus area.

Sediment supply from (high-grade) metamorphic terranes is indicated by metamorphic lithoclasts and minerals (e.g. high-Mg garnet), indicating an exposed metamorphic basement at the time of deposition. Eclogitic garnets (all Cretaceous sediments) and glaucophane (Keramaian Formation) point toward a source from a high-pressure low-temperature metamorphic terrane, typically associated with exhumed subduction complexes. An ophiolitic source is supported by the presence of chromian spinel (Keramaian Formation IK8-1) and radiolarite lithics in the Manunggul and Paniungang formations. Garnet chemistry (Fig. 7) yields a rather uniform source of the Keramaian turbidites. The chemistry of blue amphiboles is similar to glaucophane-(crossite) relicts from the nearby Aranjo/Hauran amphibolite-facies schist (Soesilo, 2012), inferring that these metamorphites were already exhumed in the Late Cretaceous. The slightly more diverse composition of the Paniungang garnets suggests two important suppliers of rather similar character, presumably metamorphic terranes of slightly different composition or grade. The large variation of garnet compositions in the Manunggul Formation indicates a wide catchment area with a large variety of different garnet suppliers, the erosion of well-mixed precursor sediments or both. The U–Pb zircon ages obtained for the Manunggul sediments also show notable variation (Fig. 3).

5.3. Detrital kimberlitic and carbonatitic zircon

The screening of our zircon trace element dataset for potentially mantle-associated zircons as described in the results Section 3.4 resulted in a subset of 51 zircons with carbonatitic affinity and 10 zircons with kimberlitic affinity (cf. Electronic Appendix 1, sheet "Carbonatitic & Kimberlitic Zircons"). A detailed comparison with the chemistry of zircons known from kimberlites shows that our screening was not able to unambiguously identify mantle-derived zircon but rather identifies eclogite-derived crystals. The interpretation for zircons with carbonatitic affinity is less clear.

Zircons labeled as "carbonatitic" show minor to non-existent negative Eu-anomalies, low REE-concentrations and moderately steep HREE patterns ($[Yb/Gd]_n$ = 8.06 to 121.4, average = 48.9, Fig. 5A). These features are similar to eclogitic zircons described from the Italian Alps or UHP-gneisses from the Kokchetav Massive in Kazakhstan (Hermann et al., 2001; Rubatto, 2002) and could therefore indicate an eclogitic origin. However, Th/U ratios > 0.17 in these zircons are atypical

Please cite this article as: Kueter, N., et al., Tracing the depositional history of Kalimantan diamonds by zircon provenance and diamond morphology studies, Lithos (2016), http://dx.doi.org/10.1016/j.lithos.2016.05.003

for high-grade metamorphic zircons and more typical for magmatic environments (Rubatto, 2002; Rubatto and Gebauer, 2000).

Zircons identified as "kimberlitic" during screening differ markedly from those with a carbonatitic affinity in having flat HREE tails ($[Yb/Gd]_n = 1.1$ to 3.7), similar to the zircons found in SCLM and kimberlites worldwide (Page et al., 2007). On the other hand, flat HREE tails in the zircons are also a typical feature of synchronous zircon and garnet growth as occurring in eclogites (Hermann et al., 2001; Rubatto, 2002 and references therein). Hence, flat HREE tails indicate high-pressure conditions but not necessarily a SCLM origin. Similarly, half of the "kimberlitic" zircons yield Th/U ratios smaller than 0.1, supporting a metamorphic origin (Rubatto and Gebauer, 2000). All of the "kimberlitic" zircons show some negative Eu-anomalies ($Eu/Eu^* = 0.06$ and $Eu/Eu^* = 0.42$–0.62) that are too pronounced compared to literature values for kimberlite zircons (average $Eu/Eu^* = 0.9 \pm 0.26\ 1\sigma$), but resemble eclogitic zircons described by Rubatto (2002) ($Eu/Eu^* = 0.24$ to 0.63).

Crystallization ages measured for the great majority of both "kimberlitic" and "carbonatitic" zircons (134 to 174 Ma) match the timing of the Cretaceous Meratus orogeny and could correspond to Meratus blueschist and granulite facies metamorphism (165–180 Ma and 135–154 Ma respectively; Parkinson et al., 1998; Soesilo, 2012; Wakita et al., 1998). During orogeny and metamorphism shallow hot asthenospheric mantle would preclude emplacement of diamondiferous kimberlites.

Rather, trace element chemistry and findings of detrital blueschist glaucophane and eclogitic garnet in the same sediment samples support an eclogitic source for zircons that were screened as "kimberlitic". These zircons may have grown in a high pressure regime during peak metamorphism of the Meratus orogeny. The interpretation of carbonatitic zircons is less clear due to their chemical and age evidence for both a magmatic and metamorphic origin.

Although this study does not provide clear evidence for kimberlitic zircon, we conclude that zircon may serve as a kimberlite indicator mineral for anomalous diamond deposits lacking common indicator minerals. Common zircon grades in kimberlites are around 1 g/t but can reach up to 50 g/t and are therefore at least as common as diamond in economy-grade kimberlites (Kresten et al., 1975). Owing to zircon resistivity against physicochemical corrosion, hydraulic properties, and high specific density, zircons accompany diamonds during alluvial sedimentation processes.

We suggest that in addition to the CART-tree method of Belousova et al. (2002), a more tedious screening of the analyses is necessary to separate igneous from metamorphic and deep-crustal from SCLM zircons. Based on literature data for kimberlitic zircon, we suggest using additional criteria of $Th/U > 0.1$ and $Eu/Eu^* > 0.7$ to separate kimberlitic zircon from eclogitic zircon.

6. Discussion - diamonds

A recent study by Smith et al. (2009) favors a subcontinental lithospheric growth-environment for Kalimantan diamonds based on the Archean ages of their sulfide inclusions, the abundant peridotitic and eclogitic silicate inclusions (70% and 30%, respectively), estimates of formation pressures and temperatures of silicate inclusions, as well as diamond nitrogen defects reflecting long-term growth and residence times in the mantle. Our crystallization pressure estimate of 4.8 and 6 GPa (calculated for 930 and 1250 °C) for a garnet inclusion lies well within the diamond stability field and plots along with other inclusion data (Smith et al., 2009) between the 35 to 41 mW/m^2 geotherms. Diamond morphologies also agree with the conclusion of a SCLM origin in a way that Kalimantan diamonds share many features of lithospheric diamonds transported to the surface by high-alkaline magma. The presence of deformation lamellae imply temperatures exceeding 900 °C with pressures corresponding to the diamond stability field (DeVries, 1975) and assume local stress fields in the areas of proto-kimberlite propagation (Gurney et al., 2004). The etch pitting style of octahedral diamond faces closely resembles kimberlite-induced and mantle-derived resorption described on natural diamonds found in kimberlites (Zhang and Fedortchouk, 2012). The etch pits often mark dislocation lines on diamond crystals (Fedortchouk et al., 2005). A special type of deep hexagonal etch channels observed on two Kalimantan Barat THH diamonds (KB 37 and KB54, Fig 8E) is also described as a frequent feature from Argyle diamonds (Sobolev et al., 1989). Diamond deformation and certain etch pitting (e.g. frosting, circular pits) have not yet been observed at non-conventional diamond localities (ophiolites, UHP-diamonds) but are typical features for diamonds formed in SCLM and emplaced by lamproitic or kimberlitic magmatism.

The small sample size precludes detailed conclusions on the diamond host environments. However, the features of the two studied diamond populations indicate a variety of resorption conditions in the mantle and the transporting magma. Abundant THH forms, di-trigonal shapes of resorbed {111}-faces, glossy appearances and circular pits often observed on the same stone are very similar to diamond features from volcaniclastic kimberlite facies elsewhere and to products of dissolution experiments in the presence of an H_2O-fluid (Fedortchouk et al., 2007, 2010). Diamonds with trigonal {111}-outlines and dodecahedral crystal forms imply a CO_2-dominated dissolution environment and resemble mantle-derived diamond resorption found in kimberlitic diamonds (Zhang and Fedortchouk, 2012). THH-forms and specimens with circular etch pitting (disks) are similar to diamond features described from kimberlites worldwide (Fedortchouk et al., 2010; McCallum et al., 1991; Robinson et al., 1989). The formation of disks is linked to volatile or melt bubbles attached to the diamond surface where they either protect it from the corrosive environment or locally etch circular depressions (Pandeya and Tolansky, 1961). In experiments, disks form at pressures below 10 kbar under H_2O-enriched conditions (Fedortchouk et al., 2007).

A large proportion of the Kalimantan diamonds show surfaces with different degrees of frosting. Fine frosting developed along the resorbed edges of octahedral and THH diamonds resembles diamond surface morphologies from coherent kimberlite facies (Fedortchouk et al., 2010), whereas coarse frosting may accompany diamond surface graphitization as was experimentally reproduced on diamonds in volatile-undersaturated or dry melts (Fedortchouk et al., 2007). A few fractured stones yield frosted cleavage-planes indicating chemical corrosion at high temperature following the breaking. It can be argued that such diamonds were fractured during the violent volcanic emplacement of a kimberlite/lamproite (Robinson, 1980).

Radiation spots and abrasion marks are indicators of an extended alluvial history of the diamonds and the presence of secondary diamond placer collectors. Their absence on some diamonds in our samples implies mixed diamond populations with different alluvial histories. The majority of the diamonds show radiation spots caused by alpha particle emission from adjoining radioactive minerals. Recent experiments by Nasdala et al. (2013) constrain the formation time of visible faint-green spots on the order of 10 myr with uranite as adjacent grain and 1.2 Ga with zircon (1000 ppm U) as an adjacent grain. Hence, any radioactive mineral with radioactivity between these two end members would require tens of millions of years of an undisturbed geological environment to produce visible spots. Trails of radiation-spots observed on some stones can be interpreted as minute relative movements between the diamond and a radiation source (Fig. 8G). Radiation coloring on diamond is initially green and turns into brown color when heated to temperatures exceeding 450 °C (Meyer et al., 1965; Nasdala et al., 2013). The brown radiation–coloration of the Kalimantan diamonds may indicate a heating event that widely affected the diamond host rocks. The high abundance of brown radiation coloring compared to a rather small quantity of green radiation spots is a common feature of all diamond occurrences in Southeast Asia (Griffin et al., 2001; Smith et al., 2009; Win et al., 2001). The strongly increased number of diamonds with radiation spots in the KB suite compared to the KS suite

Please cite this article as: Kueter, N., et al., Tracing the depositional history of Kalimantan diamonds by zircon provenance and diamond morphology studies, Lithos (2016), http://dx.doi.org/10.1016/j.lithos.2016.05.003

correlates with an increase in abrasion marks in diamonds of the KB population compared to the KS suite (c. 45% diamonds without apparent abrasion). This observation agrees with findings of Smith et al. (2009), (Fig. 3, p. 825) indicating a profound difference in 'rhombic' abrasion between South Kalimantan (c. 5%) and West Kalimantan (c. 30%). The alluvial diamond mine PT-Galuh Cempaka reported to us a strongly bimodal distribution of worn and very fresh diamonds. A complex alluvial history should provide stones of remarkable quality since bad quality stones (boart, fractured, coated or inclusion-rich stones) do not survive the prolonged transportation (Sutherland, 1982). Unworn perfect octahedral diamonds, coated diamonds (e.g. ballas), complex-shaped crystal aggregates and aggregates with unbroken (multiple) terminations and multiple inclusions are fairly common and indicate little alluvial transport (e.g. immediate storage in a paleo-collector after erosion from a primary source) or proximal liberation from a primary source within the Meratus area.

7. Depositional model: The journey of Kalimantan diamonds

7.1. Pre-rifting and rifting phase: Primary diamond sources and paleo-collectors (Precambrian–Permian)

Plate tectonic reconstructions locate the Argoland block (incl. SBW and EJT, Fig. 10) close to the northern continental margin of NW-Australia (Hall and Sevastjanova, 2012; Metcalfe, 2011). The North Australian Craton hosts several kimberlite and lamproite provinces, some of which are economic such as the Argyle lamproite famous for its pink diamonds (Hutchison, 2013; Shigley et al., 2001). These provinces were emplaced prior or during the rifting stage, and the diamonds liberated into a (nearby) paleo-collector or remained situated within their primary source. Diamonds that became part of the alluvial cycle likely mixed with diamonds of older provinces during the deposition of new placer environments.

7.2. Plate migration phase: Episode of passive diamond transport (Permian–Triassic/Jurassic)

The detachment of the Argoland block proceeded via rifting and northwards migration towards the Sundaland subcontinent in the form of smaller terranes separated by newly formed oceanic lithosphere. Formation of the Meratus ophiolite took place between the Late Triassic and Early Jurassic (Coggon et al., 2011; Wakita et al., 1998), falling into the period of active terrane migration. The alluvial sediments or magmatic sources of diamond deposits within these terranes may be covered by younger sediments so that a large proportion of diamonds remains in a geologically undisturbed environment for the next tens of millions of years gaining the radiation spots of initially green color.

7.3. Pre-collisional stage: First liberation of non-metamorphosed diamonds (Early Mesozoic)

Prior to collision, an active subduction zone demarcated the southern margin of Proto-Southeast Asia (Figs. 1, 10, "Karimunjawa-trench"), resulting in calc-alkaline magmatism within the Southwest Borneo Terrane (e.g. Schwaner Mountains). The orogeny shed sediments into a forearc setting in the paleo-south as indicated by rounded detrital zircons of the Triassic age. It is possible that diamonds liberated from their paleo-sources by earlier orogenic events were re-deposited in the forearc sediments.

7.4. Early collisional stage: Metamorphic overprint of diamond paleo-collectors (Jurassic–Early Cretaceous)

As indicated by the seismic profiles (Granath et al., 2011), the cessation of the active subduction led to underthrusting of the EJT terrane by the SWB. This process was accompanied by metamorphism of sedimentary cover including shelf and forearc sediments, and paleo-collectors (Parkinson et al., 1998; Soesilo, 2012). Previous subduction mélanges became part of the crustal stacking and were overprinted by regional metamorphism during SWB–EJT-collision (blueschist/eclogite to granulite-facies overprint observed in metamorphites in the central Meratus; Soesilo, 2012). The eastern ophiolite was obducted onto the metamorphic base. Being partly affected by the regional metamorphism, paleo-collectors as well as the primary host rocks changed their lithologies. Inherited diamonds were heated up and changed from initially green radiation–coloring to brown. This interpretation is in agreement with green cathode-luminescence observed on 59% of the diamonds described by Smith et al. (2009). Green CL-response is thought to be connected to metamorphic overprint of diamonds (Bruce et al., 2011; Yelisseyev et al., 2013). It is possible that metamorphism also erased the primary mineralogy of any preserved magmatic diamond sources. Such a case is described for the Birim diamond deposits in Ghana, where kimberlitic diamonds are found in ultramafic actinolite schists with chemical signatures of kimberlite-type rocks, whose primary mineral content was replaced during the Proterozoic Eburnean Orogeny regional metamorphism. Associated alluvial deposits are rich in diamonds but no kimberlite indicators have been reported (Appiah et al., 1996; Asiedu et al., 2004; Chirico et al., 2010; Kesse, 1985).

Placer diamonds that did not experience a metamorphic overprint became part of the alluvial cycle as soon as their sedimentary hosts were exhumed. The abraded fraction of the diamonds was subject to a prolonged alluvial transport history with multiple sedimentary cycles, while the more pristine proportion of diamonds underwent passive transportation by plate movement and were liberated from their host during the Meratus orogeny in the Cretaceous.

7.5. Late collision stage (cretaceous)

Calc-alkaline magmatism accompanied the opening of a new subduction zone approximately 300 km further paleo-south (Bantimala-trench, Fig. 1) (Soesilo, 2012) and crosscut the metamorphic and ophiolitic base of the Meratus (Pitanak Group). Continuous uplift of the collision zone exposed older sedimentary strata including allochthonous sediments from Australia and the metamorphic basement rocks. Erosion of these provenances formed the Cretaceous clastic sediments of the Alino Group. Diamonds liberated from either non-metamorphosed paleo-collectors or metamorphosed paleo-collectors and/or metakimberlites were concentrated in the newly formed clastic sediments of the Manunggul and possibly the Paniungang formations.

The increased volcanic activity in the Cenomanian to Santonian was reflected in the increase of volcaniclastic debris in the upper Manunggul Formation and the deposition of thick purely volcaniclastic sequences of the Pitanak Group (Sikumbang, 1986) and may have played an important role in preserving Austral–Gondwanaland-delivered diamond sources under a volcaniclastic cover.

7.6. Postorogenic stage (Late Cretaceous–Quaternary)

Flattening of the Meratus orogen and deposition of the predominantly volcaniclastic Manunggul Formation continued until the Early Paleocene (Sikumbang, 1986) when shallow relief and sea-level rise decelerated erosion until brought to a halt. After the middle Eocene, erosion continued while sea regression exposed the Meratus highlands. Erosion affected the diamond-bearing Cretaceous sediments, which shed the basal alluvial fans of the Tanjung Formation (Witts et al., 2012). The Eocene diamond-bearing conglomerates were partially exploited in the early 20th century by artisanal miners and became an important constituent of the Quaternary Cempaka paleo-channel alluvium (Koolhoven, 1935). Diamonds liberated late from Cretaceous

Please cite this article as: Kueter, N., et al., Tracing the depositional history of Kalimantan diamonds by zircon provenance and diamond morphology studies, Lithos (2016), http://dx.doi.org/10.1016/j.lithos.2016.05.003

and Eocene placers gained new radiation spots of green color which are often found next to older brown radio-coloration.

8. Conclusions

To constrain the origin and emplacement history of the headless Kalimantan diamonds, we combined diamond morphological descriptions with aspects of sediment provenance analysis, zircon geochronology, major element compositional mineral analyses and X-ray diffraction analysis of diamond-hosted inclusions. The majority of the diamonds experienced a classic growth history in a cratonic SCLM, followed by volcanic emplacement via a kimberlite or lamproite and liberation into a paleo-collector. It cannot be excluded that a minor proportion of the Kalimantan diamonds originated from anomalous sources like ophiolites or UHP-metamorphic terranes as evidence for UHP-metamorphics is present (eclogitic garnet and zircon). However, almost all of the diamonds studied here show resorption styles and surface features known from kimberlite-hosted diamonds worldwide.

The kalimantan diamonds as a whole have morphologies and surface features different to diamonds from the known kimberlites and lamproites of northern Australia (Hall and Smith, 1985; Sobolev et al., 1989), including Merlin (C.B. Smith, pers. com). Nevertheless, the Kalimantan diamonds share some characteristics with diamonds from the North Australian Craton. Jaques et al. (1990) reported equilibration conditions of 5–6 GPa and 1140–1290 °C for diamondiferous peridotite xenoliths from the 1180 Ma Argyle lamproite, which are in good agreement with the 1260 °C/6.04 GPa estimate of our garnet inclusion. The North Australian Craton below Argyle is also known to host comparatively large amounts of pink diamonds, which also occur in Southeast Kalimantan. Diamonds from the Argyle mine frequently show deep etch channels (Sobolev et al., 1989), a feature observed also on two resorbed diamonds from Kalimantan Barat. Signatures of the Australian orogens (e.g. Alice Springs or Halls Creek, Fig. 10) form prominent peaks in the zircon age density distributions of the Meratus clastic sediments. Especially, the diamond-bearing Manunggul Formation yields the broadest spectrum of pre-collisional zircons and the clearest presence of age densities corresponding to the King Leopold and Halls Creek orogenies. Accordingly, a sediment source with a strong link toward Northwest Australia (e.g. Kimberley or Canning Basin sediments or Australian crystalline basement, Fig. 10) must have acted as an important detritus supplier for this formation. Hence, based on the diamond and sediment data, we conclude that the great majority of Kalimantan diamonds may ultimately have a North Australian origin and share the same cratonic host as diamond deposits in northern Australia. The difference in morphology styles between the majority of the Kalimantan diamonds and the North Australian diamonds make a direct link to the known diamond occurrences (e.g. Argyle or Merlin) unlikely but favors unknown kimberlite and lamproite sources in the North Australian Craton that foundered during the collision events.

The Kalimantan diamonds were subject to a complex dispersal history driven by continental breakup and reformation of lithospheric fragments ultimately forming Southeast Asia's continental core. They were transported passively by plate migration while situated within primary sources or in paleo-placer deposits favoring also the survival of low-quality diamonds. Within their primary or secondary sources, the diamonds partly experienced regional metamorphism during episodes of terrane amalgamation that caused the transformation of initially green radiation–coloration to brown radiation spots and the elimination of kimberlite indicator minerals. Associated orogenic events exhumed diamond-bearing lithologies and subsequent erosion steadily liberated them into the local orogenic alluvial cycle. Thereby the fraction of diamonds with already existent abrasion wear (e.g. gained prior to the Gondwana breakup) mixed with the fresh-looking diamond populations liberated from primary magmatic sources or proximal paleo placers. Further, the diamonds that were liberated early into the inner-orogenic sedimentary cycle are more likely to show abrasion features, whereas diamonds situated within deeper, eventually metamorphosed host rocks were longer protected against the erosional cycle. The latter group of diamonds was continuously liberated during successive exhumation of the orogenic base, a process that still could supply unworn diamonds into recent placers today.

Our genetic model for the Kalimantan diamonds may also be applicable to other diamond deposits in Southeast Asia, as a lack of kimberlite indicator minerals and a predominance of brown radiation coloration is observed in all Southeast Asian diamond localities (Griffin et al., 2001; Win et al., 2001). All these deposits are located close to collision orogens that formed by amalgamation of continental fragments originating from the Australian part of Gondwanaland. The example of Ghana's diamond deposits show that metamorphic overprint of kimberlite-type rocks and the associated loss of indicative minerals are possible without destroying the actual diamond content. Metamorphic processes could not only be responsible for changes in the color of radiation spots and the elimination of kimberlite indicator minerals, but also for changes in cathodoluminescence colors from primary bluish to green, yellow and orange colors as reported by Smith et al. (2009).

The X-ray diffraction inclusion analysis offers a way to elucidate growth conditions on diamonds and obtain qualitative chemical composition of entrapped minerals when the physical exposure of an inclusion is not possible. This non-invasive technique is particularly advantageous for the investigation of anomalous diamond deposits where sample material requires special care (e.g. when in the property of private collectors or museums) or sample material is rare and hence should be preserved (e.g. Californian or Myanmar diamonds, cf. Griffin et al., 2001; Kopf et al., 1990; Win et al., 2001).

Exploration for diamond sources for headless deposits in geological settings that have experienced metamorphic events requires alternative indicators such as zircon. The morphology, physical characteristics and trace-element chemistry of kimberlitic zircon is distinct from crustal zircons (Belousova et al., 1998, 2002; Fedo et al., 2003; Hoskin and Ireland, 2000; Kresten et al., 1975; Page et al., 2007; Zheng et al., 2006). This study has shown that discrimination of zircon is possible, but found no indubitable kimberlite zircons in our samples. Since the Southeast Kalimantan diamond deposit is situated close to a collisional orogen, zircons grown within subduction-associated high-pressure rocks became part of the diamondiferous sediments. For such settings, datasets of potential kimberlitic zircons have to be screened for eclogite-derived zircons by examining the dataset for U/Th and Eu/Eu* ratios. Further zircon studies including mineral inclusions, $\delta^{18}O$ and Hf-isotope analyses could identify a true kimberlitic origin within an SCLM. Once clearly identified as kimberlite-derived, the zircons real merit will lie in the estimation of a kimberlite eruption age using (U–Th–Pb)/He double-dating technique (McInnes et al., 2009). However, even when kimberlitic zircon cannot clearly be identified, we show that zircon provenance analysis can be a powerful tool for unraveling the depositional history of diamondiferous and related sediments and may help to constrain the source region.

Uncited reference

Q6

Miyashiro, 1957

Acknowledgement

Ir. Kuncoro Hadi and Ir. Bob Nugroho from the PT Galuh Cempaka diamond mine (Banjabaru) kindly shared their expertise and provided heavy mineral samples. Adip Mustofa (Lambung Mangkurat University, Banjarmasin) and Gimin (Martapura) are gratefully thanked for discussions and field accompany. Aminruddin and the Geological Survey in Bandung contributed knowledge and literature. We thank Karsten Kunze from ScopeM at ETH Zurich (www.scopem.ethz.ch) for his assistance with cathodoluminescence imaging. Maya Kopylova (University of British Columbia), Ben Ellis and Jakub Sliwinsky (both ETH Zurich)

Please cite this article as: Kueter, N., et al., Tracing the depositional history of Kalimantan diamonds by zircon provenance and diamond morphology studies, Lithos (2016), http://dx.doi.org/10.1016/j.lithos.2016.05.003

are thanked for valuable discussions and help. We thank Ross J. Angel (Università degli Studi di Padova) for the manuscript review. Chris Smith (University of Bristol) and an anonymous reviewer are thanked for their valuable suggestions to this manuscript. The geochemical plots were drafted with the Geochemical Data Toolkit (Janousek et al., 2006).

This work was financially supported by an ETH student project scholarship and by the European Research Council Starting Grant to FN (agreement no. 307322).

Appendix A. Supplementary data

Supplementary data to this article can be found online at http://dx.doi.org/10.1016/j.lithos.2016.05.003.

References

Angel, R.J., Nestola, F., 2015. A century of mineral structures: how well do we know them? American Mineralogist (sumitted).
Angel, R.J., Alvaro, M., Gonzalez-Platas, J., 2014a. EosFit7c and a Fortran module (library) for equation of state calculations. Zeitschrift für Kristallographie-Crystalline Materials 229, 405–419.
Angel, R.J., Alvaro, M., Nestola, F., Mazzucchelli, M.L., 2015b. Diamond thermoelastic properties and implications for determining the pressure of formation of diamond-inclusion systems. Russian Geology and Geophysics 56, 211–220.
Angel, R.J., Mazzucchelli, M.L., Alvaro, M., Nimis, P., Nestola, F., 2014b. Geobarometry from host-inclusion systems: the role of elastic relaxation. American Mineralogist 99, 2146–2149.
Angel, R., Nimis, P., Mazzucchelli, M., Alvaro, M., Nestola, F., 2015a. How large are departures from lithostatic pressure? Constraints from host–inclusion elasticity. Journal of Metamorphic Geology.
Appiah, H., Norman, D., Kuma, J., 1996. The diamond deposits of Ghana. Africa Geoscience Review 3, 261–272.
Asiedu, D., Dampare, S., Sakyi, P.A., Banoeng-Yakubo, B., Osae, S., Nyarko, B., Manu, J., 2004. Geochemistry of Paleoproterozoic metasedimentary rocks from the Birim diamondiferous field, southern Ghana: implications for provenance and crustal evolution at the Archean–Proterozoic boundary. Geochemical Journal-Japan 38, 215–228.
Baese, R., 2013. Fluid–Rock Interaction Processes during Subduction and Exhumation of Oceanic Crust: Constraints from Jadeitites in Serpentinites, Eclogite Veins in Blueschists and Tectonic Breccias Formed during Uplift. Institut für Geowissenschaften. Christian-Albrechts-Universität, Kiel (Diss., 2012).
Barron, L., Mernagh, T., Barron, B., Pogson, R., 2011. Spectroscopic research on ultrahigh pressure (UHP) macrodiamond at Copeton and Bingara NSW, Eastern Australia. Spectrochimica Acta Part A: Molecular and Biomolecular Spectroscopy 80, 112–118.
Barron, L., Mernagh, T., Pogson, R., Barron, B., 2008. Alluvial ultrahigh pressure (UHP) macrodiamond at Copeton/Bingara (Eastern Australia), and Cempaka (Kalimantan, Indonesia). 9th International Kimberlite Conference, Extended Abstract, 9IKC-A-00039, pp. 1–3.
Belousova, E.A., Griffin, W.L., O'Reilly, S.Y., Fisher, N.I., 2002. Igneous zircon: trace element composition as an indicator of source rock type. Contributions to Mineralogy and Petrology 143, 602–622.
Belousova, E., Griffin, W., Pearson, N., 1998. Trace element composition and cathodoluminescence properties of southern African kimberlitic zircons. Mineralogical Magazine 62, 355–366.
Bergman, S.C., Dunn, D.P., Krol, L.G., 1988. Rock and mineral chemistry of the Linhaisai Minette, Central Kalimantan, Indonesia, and the origin of Borneo diamonds. The Canadian Mineralogist 26, 23–43.
Bruce, L.F., Kopylova, M.G., Long, M., Ryder, J., Dobrzhinetskaya, L.F., 2011. Luminescence of diamonds from metamorphic rocks. American Mineralogist 96, 14–22.
Buick, I., Storkey, A., Williams, I., 2008. Timing relationships between pegmatite emplacement, metamorphism and deformation during the intra-plate Alice Springs Orogeny, Central Australia. Journal of Metamorphic Geology 26, 915–936.
Canil, D., Mihalynuk, M., MacKenzie, J., Johnston, S., Grant, B., 2005. Diamond in the Atlin Nakina region, British Columbia: insights from heavy minerals in stream sediments. Canadian Journal of Earth Sciences 42, 2161–2171.
Casselman, S., Harris, B., 2002. Yukon Diamond Rumor Map and Notes. Aurora Geosciences Ltd. and Energy, Mines and Resources, Government of Yukon, p. 1.
Chirico, P.G., Malpeli, K.C., Anum, S., Phillips, E.C., 2010. Alluvial diamond resource potential and production capacity assessment of Ghana. US Geological Survey Scientific Investigations Report 2010, p. 5045.
Clements, B., Burgess, P.M., Hall, R., Cottam, M.A., 2011. Subsidence and uplift by slab-related mantle dynamics: a driving mechanism for the Late Cretaceous and Cenozoic evolution of continental SE Asia? Geological Society–Special Publications 355, 37–51.
Coggon, J.A., Nowell, G.M., Pearson, D.G., Parman, S.W., 2011. Application of the ^{190}Pt–^{186}Os isotope system to dating platinum mineralization and ophiolite formation: an example from the Meratus Mountains, Borneo. Economic Geology 106, 93–117.
Davies, G., Evans, T., 1972. Graphitization of diamond at zero pressure and at a high pressure. Proceedings of the Royal Society of London. Series A: Mathematical and Physical Sciences 413–427.
Davies, G.R., Nixon, P.H., Pearson, D.G., Obata, M., 1993. Tectonic implications of graphitized diamonds from the Ronda Peridotite Massif, southern Spain. Geology 21, 471–474.
Davies, R.M., O'Reilly, S.Y., Griffin, W.L., 2002. Multiple origins of alluvial diamonds from New South Wales, Australia. Economic Geology 97, 109–123.
DeVries, R., 1975. Plastic deformation and "work-hardening" of diamond. Materials Research Bulletin 10, 1193–1199.
Dirk, M.H.J., Amiruddin, 2000. Batuan granitoid. Evolusi Magmatic Kalimantan Selatan. PSG Special publication Vol. 23.
Dymshits, A.M., Litasov, K.D., Sharygin, I.S., Shatskiy, A., Ohtani, E., Suzuki, A., Funakoshi, K., 2014. Thermal equation of state of majoritic knorringite and its significance for continental upper mantle. Journal of Geophysical Research–Solid Earth 119, 8034–8046.
Fedo, C.M., Sircombe, K.N., Rainbird, R.H., 2003. Detrital zircon analysis of the sedimentary record. Reviews in Mineralogy and Geochemistry 53, 277–303.
Fedortchouk, Y., Canil, D., Carlson, J.A., 2005. Dissolution forms in Lac de Gras diamonds and their relationship to the temperature and redox state of kimberlite magma. Contributions to Mineralogy and Petrology 150, 54–69.
Fedortchouk, Y., Canil, D., Semenets, E., 2007. Mechanisms of diamond oxidation and their hearing on the fluid composition in kimberlite magmas. American Mineralogist 92, 1200–1212.
Fedortchouk, Y., Matveev, S., Carlson, J.A., 2010. H_2O and CO_2 in kimberlitic fluid as recorded by diamonds and olivines in several Ekati Diamond Mine kimberlites, northwest territories, Canada. Earth and Planetary Science Letters 289, 549–559.
Festa, A., Pini, G.A., Dilek, Y., Codegone, G., 2010. Melanges and melange-forming processes: a historical overview and new concepts. International Geology Review 52, 1040–1105.
Granath, J.W., Christ, J.M., Emmet, P.A., Dinkelman, M.G., 2011. Pre-Cenozoic sedimentary section and structure as reflected in the JavaSPAN (TM) crustal-scale PSDM seismic survey, and its implications regarding the basement terranes in the East Java Sea. Geological Society–Special Publications 355, 53–74.
Griffin, W.L., Win, T.T., Davies, R., Wathanakul, P., Andrew, A., Metcalfe, I., Cartigny, P., 2001. Diamonds from Myanmar and Thailand: characteristics and possible origins. Economic Geology and the Bulletin of the Society of Economic Geologists 96, 159–170.
Grütter, H.S., Gurney, J.J., Menzies, A.H., Winter, F., 2004. An updated classification scheme for mantle-derived garnet, for use by diamond explorers. Lithos 77, 841–857.
Guillong, M., Meier, D., Allan, M., Heinrich, C., Yardley, B., 2008. SILLS: a MATLAB-based program for the reduction of laser ablation ICP-MS data of homogeneous materials and inclusions. Mineralogical Association of Canada Short Course 40, 328–333.
Gurney, J.J., Hildebrand, P.R., Carlson, J.A., Fedortchouk, Y., Dyck, D.R., 2004. The morphological characteristics of diamonds from the Ekati property, northwest territories, Canada. Lithos 77, 21–38.
Haile, N.S., McElhinny, M.W., McDougall, I., 1977. Palaeomagnetic data and radiometric ages from the Cretaceous of West Kalimantan (Borneo), and their significance in interpreting regional structure. Journal of the Geological Society of London 133–144.
Haines, P.W., Hand, M., Sandiford, M., 2001. Palaeozoic synorogenic sedimentation in central and northern Australia: a review of distribution and timing with implications for the evolution of intracontinental orogens. Australian Journal of Earth Sciences 48, 911–928.
Hall, R., Sevastjanova, I., 2012. Australian crust in Indonesia. Australian Journal of Earth Sciences 59, 827–844.
Hall, A.E., Smith, C.B., 1985. Lamproite Diamonds—Are They Different? University of Western Australia, Geology. Dept
Hanchar, J., Hoskin, P., 1998. Mud Tank carbonatite, Australia, zircon. Society for Luminescence Microscopy and Spectroscopy Newsletter 10, 2–3.
Hashimoto, W., Koike, T., 1973. A geologic reconnaissance of the reservoir area of the Riam Kanan Dam, east of Martapura Kalimantan Selatan. Geology and Paleontology in Southeast Asia 13, 163–185.
Hausel, W.D., 2007. Diamonds & Mantle Source Rocks in the Wyoming Craton (with Discussions on the North American Craton & Unconventional Source Terrains). W. Dan Hausel Geological Consulting LLC.
Hermann, J., Rubatto, D., Korsakov, A., Shatsky, V.S., 2001. Multiple zircon growth during fast exhumation of diamondiferous, deeply subducted continental crust (Kokchetav Massif, Kazakhstan). Contributions to Mineralogy and Petrology 141, 66–82.
Hollis, J.A., Carson, C.J., Glass, L.M., 2009. SHRIMP U–Pb zircon geochronological evidence for Neoarchean basement in western Arnhem Land, northern Australia. Precambrian Research 174, 364–380.
Hoskin, P.W.O., Ireland, T.R., 2000. Rare earth element chemistry of zircon and its use as a provenance indicator. Geology 28, 627–630.
Howell, D., Wood, I.G., Nestola, F., Nimis, P., Nasdala, L., 2012. Inclusions under remnant pressure in diamond: a multi-technique approach. European Journal of Mineralogy 24, 563–573.
Hubert, J.F., 1962. A zircon–tourmaline–rutile maturity index and the interdependence of the composition of heavy mineral assemblages with the gross composition and texture of sandstones. Journal of Sedimentary Research 32.
Hutchison, M.T., 2013. Diamond exploration and regional prospectivity of the northern territory of Australia. Proceedings of 10th International Kimberlite Conference. Springer, pp. 257–280.
Janousek, V., Farrow, C.M., Erban, V., 2006. Interpretation of whole-rock geochemical data in igneous geochemistry: introducing Geochemical Data Toolkit (GCDkit). Journal of Petrology 47, 1255–1259.
Jaques, A.L., O'Neill, H.S., Smith, C.B., Moon, J., Chappell, B.W., 1990. Diamondiferous peridotite xenoliths from the Argyle (Ak1) lamproite pipe, western-Australia. Contributions to Mineralogy and Petrology 104, 255–276.
Kesse, G.O., 1985. The Mineral and Rock Resources of Ghana.

Koolhoven, W., 1935. Het primaire voorkomen van den Zuid Borneo diamant. Geologische Mijnbouw Genootschaap, Verhandelingen, Geologie Serie 11, 189–232.

Kopf, R., Hurlbut, C., Koivula, J., 1990. Recent discoveries of large diamonds in Trinity County, California. Gems and Gemology 26, 212–219.

Kresten, P., Fels, P., Berggren, G., 1975. Kimberlitic zircons—a possible aid in prospecting for kimberlites. Mineralium Deposita 10, 47–56.

Krol, L., 1920. Over de geologie: van een gedeelte van de zuider-en oosterafdeeling van Borneo.

Laiginhas, F., Pearson, D.G., Phillips, D., Burgess, R., Harris, J.W., 2009. Re–Os and $^{40}Ar/^{39}Ar$ isotope measurements of inclusions in alluvial diamonds from the Ural Mountains: constraints on diamond genesis and eruption ages. Lithos 112, 714–723.

Locock, A.J., 2008. An Excel spreadsheet to recast analyses of garnet into end-member components, and a synopsis of the crystal chemistry of natural silicate garnets. Computers and Geosciences 34, 1769–1780.

Mange, M.A., Maurer, H., 2012. Heavy Minerals in Colour. Springer Science & Business Media.

Mange, M.A., Morton, A.C., 2007. Geochemistry of heavy minerals. Developments in Sedimentology 58, 345–391.

Martens, J.H.C., 1932. Piperine as an immersion medium in sedimentary petrography. American Mineralogist 17, 198–199.

McCallum, M., Huntley, P., Falk, R., Otter, M., 1991. Morphological, resorption and etch feature trends of diamonds from kimberlite populations within the Colorado–Wyoming state line district, USA. Proceedings of the 5th International Kimberlite Conference, Brasilia, Brazil, Companhia de Pesquisa de Recursos Minerals, pp. 78–97.

McDonough, W.F., Sun, S.S., 1995. The composition of the Earth. Chemical Geology 120, 223–253.

McInnes, B.I.A., Evans, N.J., McDonald, B.J., Kinny, P.D., Jakimowicz, J., 2009. Zircon U–Th–Pb–He double dating of the Merlin kimberlite field, northern territory, Australia. Lithos 112, 592–599.

Metcalfe, I., 1988. Origin and assembly of south-east Asian continental terranes. Geological Society, London, Special Publications 37, 101–118.

Metcalfe, I., 2011. Tectonic framework and Phanerozoic evolution of Sundaland. Gondwana Research 19, 3–21.

Meyer, H., Milledge, H., Nave, E., 1965. Natural Irradiation Damage in Ivory Coast Diamonds.

Milani, S., Nestola, F., Alvaro, M., Pasqual, D., Mazzucchelli, M.L., Domeneghetti, M.C., Geiger, C.A., 2015. Diamond-garnet geobarometry: the role of garnet compressibility and expansivity. Lithos 227, 140–147.

Miyashiro, A., 1957. The chemistry, optics and genesis of the alkali-amphiboles. Journal of the Faculty of Science, University of Tokyo 11, 57–83.

Monnier, C., Polve, M., Girardeau, J., Pubellier, M., Maury, R.C., Bellon, H., Permana, H., 1999. Extensional to compressive Mesozoic magmatism at the SE Eurasia margin as recorded from the Meratus ophiolite (SE Borneo, Indonesia). Geodinamica Acta 12, 43–55.

Myers, J.S., Shaw, R.D., Tyler, I.M., 1996. Tectonic evolution of Proterozoic Australia. Tectonics 15, 1431–1446.

Nasdala, L., Grambole, D., Wildner, M., Gigler, A.M., Hainschwang, T., Zaitsev, A.M., Harris, J.W., Milledge, J., Schulze, D.J., Hofmeister, W., Balmer, W.A., 2013. Radio-colouration of diamond: a spectroscopic study. Contributions to Mineralogy and Petrology 165, 843–861.

Nestola, F., Nimis, P., Ziberna, L., Longo, M., Marzoli, A., Harris, J.W., Manghnani, M.H., Fedortchouk, Y., 2011a. First crystal-structure determination of olivine in diamond: composition and implications for provenance in the Earth's mantle. Earth and Planetary Science Letters 305, 249–255.

Nestola, F., Pasqual, D., Smyth, J., Novella, D., Secco, L., Manghnani, M., Negro, A.D., 2011b. New accurate elastic parameters for the forsterite–fayalite solid solution. American Mineralogist 96, 1742–1747.

Nixon, P., Bergman, S., 1987. Anomalous occurrences of diamond. Indiaqua 47, 21–27.

Page, F.Z., Fu, B., Kita, N.T., Fournelle, J., Spicuzza, M.J., Schulze, D.J., Viljoen, F., Basei, M.A., Valley, J.W., 2007. Zircons from kimberlite: new insights from oxygen isotopes, trace elements, and Ti in zircon thermometry. Geochimica et Cosmochimica Acta 71, 3887–3903.

Pandeya, D., Tolansky, S., 1961. Micro-disk patterns on diamond dodecahedra. Proceedings of the Physical Society 78, 12.

Parkinson, C.D., Miyazaki, K., Wakita, K., Barber, A.J., Carswell, D.A., 1998. An overview and tectonic synthesis of the pre-Tertiary very-high-pressure metamorphic and associated rocks of Java, Sulawesi and Kalimantan, Indonesia. Island Arc 7, 184–200.

Pearson, D., Davies, G., Nixon, P., Milledge, H., 1989. Graphitized Diamonds from A Peridotite Massif in Morocco and Implications for Anomalous Diamond Occurrences.

Robinson, D.N., 1979/1980. Surface Textures and Other Features of Diamonds. University of Cape Town.

Robinson, D., Scott, J., Van Niekerk, A., Anderson, V., 1989. The sequence of events reflected in the diamonds of some southern African kimberlites. Kimberlites and Related Rocks 2, 990–1000.

Rubatto, D., 2002. Zircon trace element geochemistry: partitioning with garnet and the link between U–Pb ages and metamorphism. Chemical Geology 184, 123–138.

Rubatto, D., Gebauer, D., 2000. Use of cathodoluminescence for U–Pb zircon dating by ion microprobe: some examples from the western Alps. Cathodoluminescence in Geosciences 373–400.

Schulze, D.J., 2003. A classification scheme for mantle-derived garnets in kimberlite: a tool for investigating the mantle and exploring for diamonds. Lithos 71, 195–213.

Sevastjanova, I., Clements, B., Hall, R., Belousova, E.A., Griffin, W.L., Pearson, N., 2011. Granitic magmatism, basement ages, and provenance indicators in the Malay Peninsula: insights from detrital zircon U–Pb and Hf-isotope data. Gondwana Research 19, 1024–1037.

Shigley, J.E., Chapman, J., Ellison, R.K., 2001. Discovery and mining of the Argyle diamond deposit, Australia. Gems and Gemology 37, 26–41.

Sikumbang, N., 1986. The Geology and Tectonics of the Meratus Mountains South Kalimantan, Indonesia. Marine Geological Institute. Directorate General Geology and Mineral Resources, Department of Mines and Energy, Bandung, p. 142.

Sikumbang, N., Heryanto, R., 1994. Peta Geologi Lembar Banjarmasin 1712. Sekala, Kalimantan, p. 1.

Sláma, J., Košler, J., Condon, D.J., Crowley, J.L., Gerdes, A., Hanchar, J.M., Horstwood, M.S., Morris, G.A., Nasdala, L., Norberg, N., 2008. Plešovice zircon—a new natural reference material for U–Pb and Hf isotopic microanalysis. Chemical Geology 249, 1–35.

Smith, C.B., Bulanova, G.P., Kohn, S.C., Milledge, H.J., Hall, A.E., Griffin, B.J., Pearson, D.G., 2009. Nature and genesis of Kalimantan diamonds. Lithos 112, 822–832.

Smyth, H.R., Hamilton, P.J., Hall, R., Kinny, P.D., 2007. The deep crust beneath island arcs: inherited zircons reveal a Gondwana continental fragment beneath East Java, Indonesia. Earth and Planetary Science Letters 258, 269–282.

Sobolev, N.V., Galimov, E.M., Smith, C.B., Yefinova, E.S., Maltsev, K.A., Hall, A.E., Usova, L.V., 1989. Comparative study of morphology, inclusions and carbon isotope composition of diamonds in alluvials of the king George River and argyle lamproite mine (Western Australia), and of cube microdiamonds from northern Australia. Geologia i Geofizika (Soviet Geology and Geophysics) 3–18.

Soesilo, J., 2012. Cretaceous Paired Metamorphic Belts in Southeast Sundaland. Bandung Institute of Technology Indonesia.

Soesilo, J., 2015. The Mesozoic tectonic setting of SE Sundaland based on metamorphic evolution. Proceedings—Indonesian Petroleum Association Thirty-Ninth Annual Convention % Exhibition.

Spencer, L., Dikinis, S.D., Keller, P.C., Kane, R.E., 1988. The diamond deposits of Kalimantan, Borneo. Gems and Gemology 24, 67–80.

Sutherland, D.G., 1982. The transport and sorting of diamonds by fluvial and marine processes. Economic Geology 77, 1613–1620.

Taylor, W.R., Jaques, A.L., Ridd, M., 1990. Nitrogen-defect aggregation characteristics of some Australasian diamonds—time–temperature constraints on the source regions of pipe and alluvial diamonds. American Mineralogist 75, 1290–1310.

Tindle, A., Webb, P., 1994. PROBE-AMPH—a spreadsheet program to classify microprobe-derived amphibole analyses. Computers and Geosciences 20, 1201–1228.

Tyler, I., Griffin, T., 1990. Structural development of the King Leopold Orogen, Kimberley region, Western Australia. Journal of Structural Geology 12, 703–714.

Tyler, I.M., Hocking, R.M., Haines, P.W., 2012. Geological evolution of the Kimberley region of western Australia. Episodes-Newsmagazine of the International Union of Geological Sciences 35, 298.

van Bemmelen, R.W., 1949. The Geology of Indonesia: General Geology of Indonesia and Adjacent Archipelagoes, the East Indies, Inclusive of the British Part of Borneo, the Malay Peninsula, the Philippine Islands, Eastern New Guinea, Christmas Island, and the Andaman and Nicobar Islands. US Government Printing Office.

van Hattum, M.W.A., Hall, R., Pickard, A.L., Nichols, G.J., 2006. Southeast Asian sediments not from Asia: provenance and geochronology of north Borneo sandstones. Geology 34, 589–592.

Vermeesch, P., 2012. On the visualisation of detrital age distributions. Chemical Geology 312, 190–194.

Wakita, K., Miyazaki, K., Zulkarnain, I., Sopaheluwakan, J., Sanyoto, P., 1998. Tectonic implications of new age data for the Meratus complex of South Kalimantan, Indonesia. Island Arc 7, 202–222.

Williams, P., Johnston, C., Almond, R., Simamora, W., 1988. Late Cretaceous to early Tertiary structural elements of West Kalimantan. Tectonophysics 148, 279–297.

Win, T.T., Davies, R.M., Griffin, W.L., Wathanakul, P., French, D.H., 2001. Distribution and characteristics of diamonds from Myanmar. Journal of Asian Earth Sciences 19, 563–577.

Winkler, W., Bernoulli, D., 1986. Detrital high-pressure/low-temperature minerals in a late Turonian flysch sequence of the eastern Alps (western Austria): implications for early Alpine tectonics. Geology 14, 598–601.

Witts, D., Hall, R., Nichols, G., Morley, R., 2012. A new depositional and provenance model for the Tanjung Formation, Barito Basin, SE Kalimantan, Indonesia. Journal of Asian Earth Sciences 56, 77–104.

Yang, J.S., Robinson, P.T., Dilek, Y., 2014. Diamonds in ophiolites. Elements 10, 127–130.

Yelisseyev, A., Afanasiev, V., Kopylova, M., Bulbak, T., 2013. The effect of electron irradiation and metamorphic annealing on optical properties of Type IaA diamonds. The Canadian Mineralogist 51, 439–453.

Yuwono, Y., Priyomarsono, S., Maury, t.R., Rampnoux, J., Soeria-Atmadja, R., Bellon, H., Chotin, P., 1988. Petrology of the Cretaceous magmatic rocks from Meratus Range, Southeast Kalimantan. Journal of Southeast Asian Earth Sciences 2, 15–22.

Zhang, Z., Fedortchouk, Y., 2012. Records of mantle metasomatism in the morphology of diamonds from the Slave craton. European Journal of Mineralogy 24, 619–632.

Zheng, J., Griffin, W., O'Reilly, S.Y., Yang, J., Zhang, R., 2006. A refractory mantle protolith in younger continental crust, east-central China: age and composition of zircon in the Sulu ultrahigh-pressure peridotite. Geology 34, 705–708.

Please cite this article as: Kueter, N., et al., Tracing the depositional history of Kalimantan diamonds by zircon provenance and diamond morphology studies, Lithos (2016), http://dx.doi.org/10.1016/j.lithos.2016.05.003

Tracing the depositional history of Kalimantan diamonds by zircon 2 provenance and diamond morphology studies

ORIGINALITY REPORT

8%	8%	0%	2%
SIMILARITY INDEX	INTERNET SOURCES	PUBLICATIONS	STUDENT PAPERS

PRIMARY SOURCES

1	www.gcdkit.org Internet Source	2%
2	secure.kaiserresearch.com Internet Source	2%
3	www.vangorselslist.com Internet Source	2%
4	pure.royalholloway.ac.uk Internet Source	2%

Exclude quotes	On	Exclude matches	< 2%
Exclude bibliography	Off		